Pre-bloom dynamics of the Subpolar North Atlantic microbial food web

Maria Lund Paulsen

February 18^{th} 2013

Joint Nordic Master's Programme in Marine Ecosystems and Climate
with a chosen specialization in marine biology

Preface

My thesis work was done in collaboration between Bergen University, Marine Microbiology department, supervisor Frede Thingstad and DTU-Aqua, department of marine ecology and climate, supervisor Torkel Gissel Nielsen. I participated in a cruise onboard RV Meteor from March 19^{th} to May 2^{st}- 2012, founded by EURO-BASIN. The focus of the cruise was Deep Convection, with 28 scientists working mainly on zooplankton, phytoplankton and ocean chemistry. Unfortunately some cruise data, which can be considered of importance to our study, have not yet become available, e.g. vertical velocities, POC, surface PAR, primary production and zooplankton abundance. I have here extensively used the DOC measurements done by Dennis A. Hansell, and data of phytoplankton composition analysed by Chris Daniels.

I have had the opportunity to work closely with PhD student Karen Riisgaard, when planning the work on board, and making the experimental design. I also enjoyed her company on the first leg of the cruise. After the cruise, Karen analysed most of the Lugol-preserved samples, while I measured all flow cytometer samples. I have so far done most of the data analysis and all text in this master thesis is written solely by me. This master thesis has been a great opportunity for me to get familiar with different methods as well as practical work on a cruise. I am thankful for all the help I have received. In Bergen, Aud Larsen, helped me numerous times with the flow cytometer, Jessica Ray in the laboratory and Evy Skjoldal were a great help with the packing and transportation of equipment. In Denmark, I had the great opportunity to actually look into our samples with my own eyes: via epifluorescence microscopy, with help from Helge Abildhauge Thomsen; and again with help from Karen, I learned to recognize different microzooplankton and counted numerous samples in inverted light microscope.

The work from the cruise has so far been presented at EURO-BASIN Mid-term Workshop in Lisbon, Ocean-Life annual meeting, 17^{th} Danske Havforskermøde and Nordic Climate Fish 2nd Conference. Also it has lead to two semi-scientific publications (see below) and two in coming up in the online magazines Copenhagen University Post andVidenskab.dk .

Paulsen, M.L. (2012). Speciale på Nordatlantens bølger.SCIENT9:26-27

Paulsen, M.L., Riisgaard, K., Agersted, M.D. Reeh, L., & Nielsen, T.G. (2012). Havets plankton bremser klimaændringer.Aktuel Naturvidenskab 6:36-41

Acknowledgements

First of all I want to thank Karen Riisgaard, who has taught me incredibly much, and has been a great partner and friend through countless hours of work. A lot of gratitude goes to my supervisors: Frede Thingstad, for valuable discussions, and Torkel Gissel Nielsen, for giving me amazing opportunities, great company and support. I am very grateful they made this collaboration possible, as I could not have wished for a more motivating, challenging or interesting master thesis.

I would like to thank my master program MARECLIM for two amazing years at the Universities of Bergen, Iceland, Faroe Island and Aarhus. Especially thank you to Corrina Schrum, for coordinating the program, and for giving me 6 months extension so I was able to join the cruise and do this master thesis.

For encouraging talks and great inputs: Antonio Cuevas, Lena Seuthe, Svein Rune Erga, Aud Larsen, Svein Sundby, Yngve Børsheim, Hjálmar Hátun, Polly G. Hill, Mathias Middelboe, Tom Anderson, and Mick Follows.

Big thanks to EURO-BASIN as the funding source, and the crew on board the RV Meteor on the Deep Convection Cruise, especially Françoise Morison (for great energy and preforming interesting dilution experiments as well as valuable discussions and proof-reading), Chris Daniels (for always singing with me and teaching me to use Prism), Christian Lindemann (for collaborating on measuring bacterial respiration), Lene Pankoke (for always helping me in the lab. and teaching me to use LyX), Mario Esposito (for taking the extra effort to measure nutrients from our microcosm experiments).

Last but not least, I thank my amazing boyfriend Oliver, for supporting me and always making my life full of laughter.

Contents

1 Abstract

The aim of this study was to investigate the microbial planktonic food web in the pre-bloom period of the Subpolar North Atlantic Ocean. Through repeated visits to the Icelandic Basin, Norwegian Basin, and on the Shetland Shelf in the period March 28^{th} to May 1^{st}, we recorded the abundance of all the functional groups of both autotrophic and heterotrophic microbes. At the first visits, all stations were characterized by low concentrations of chlorophyll *a* (<0.1-0.5 μg l^{-1}) and a low abundance of heterotrophic bacteria (2-3.4 $\times$ 10^5 cells ml^{-1}), heterotrophic nanoflagellates (22-84 cells ml^{-1}), ciliates (1-2 cells ml^{-1}), and heterotrophic dinoflagellates (0.1-0.3 cells ml^{-1}) within the upper mixed layer. Following the abundance of heterotrophic protists generally increased; 2-fold for bacteria and up to 5-fold for heterotrophic nanoflagellates. An initial dominance of pico eukaryotes within the phytoplankton community was observed in late winter. This was followed, however, by a significant decrease during the pre-bloom period, despite high nutrient concentrations and increasing light intensity. The decrease of pico eukaryote was concurrent with an increase of heterotrophic nanoflagellates, hence grazing pressure.

The microbial trophic interactions were analysed further via grazing experiments, performed with water sampled at the Icelandic Basin. These revealed heterotrophic nanoflagellate removal rates of 10-20 % of bacterial standing stock d^{-1} and as high as 30-50 % of the standing stock of pico phytoplankton d^{-1} in the euphotic zone. We conclude that heterotrophic nanoflagellates in the pre-bloom can satisfy up to half of their carbon demand by herbivory, and thus the strong focus of heterotrophic nanoflagellates' role, as being mainly bacterivorous, should be revised.

We document that the pre-bloom is a productive period with carbon entering the ocean food web largely via the microbial food web. Thus, not only the seasonal changes of physical condition, but also the microbial dynamics in the pre-bloom phase, are central in setting the scene for the spring bloom.

Key words: Microbial food web · Pre-bloom · Pico eukaryotes · Heterorophic nanoflagellates · Bacteria · Grazing · Deep convection · Subpolar North Atlantic

2 Introduction

Understanding the carbon/energy fluxes and trophic interactions in the plankton ecosystem is far from a trivial task. Years of discoveries, advancing techniques, and speculations have brought us closer, but several questions remain to be answered. Certain discoveries, which are essential for the focus of this study, led to the understanding that the microbial communities play a fundamental role in mediating fluxes of carbon and nutrients in marine ecosystems.

40 years ago, Steele (1974) found it difficult to reconcile how yearly primary production estimates could feed both the pelagic and benthic heterotrophs, and sustain fish catches (even when bacterial respiration was ignored from the carbon budget). It was already then speculated whether carbon that was "lost" by excretions from phyto- and zooplankton via heterotrophic bacteria and following consumption by heterotrophic protists could link to larger zooplankton, but few suitable protists capable of grazing on bacteria were known. Sorokin (1977) showed that bacteria account for more than half of community respiration, and that microzooplankton (μZP) respire twice more than mesozooplankton (MZP). Thus he confirmed the importance of microorganisms, and pointed out that these cannot be ignored from models describing ocean energy balance. Later, Fenchel (1982) described the heterotrophic nanoflagellates as major consumers of marine bacteria and finally, Azam et al., (1983) established the concept of the microbial loop and presented evidence of energy transfer via dissolved organic matter (DOM) to higher trophic levels in a linear heterotrophic food chain via bacteria, heterotrophic nanoflagellates (HNF), and μZP, establishing the concept of "microbial loop". A unique way of "looping" otherwise non-available energy in form of DOM further up the food chain.

The microbial path is, however, considered to be energetically inefficient, with only little (2 %) energy transfer to higher trophic levels (Ducklow et al., 1983), caused by the low growth efficiency (10-15 %) of marine bacteria (del Giorgio and Cole 2000) and sloppy feeding by heterotrophic nanoflagellates (Nagata, 2000). Still, as the amount of carbon bound in DOM is about 200 times greater than marine biomass (Hansell et al., 2009), carbon flow into bacteria is evidently a major pathway in marine systems: in a large part of the ocean this is the only energy source, e.g. dissolved organic carbon (DOC) is actively degraded, and important for sustaining life in the deep-ocean (Bendtsen et al., 2002). Future studies need to focus on understanding of the availability and qualities of this excessive pool of dissolved organic matter. Progress also needs to

be made in order to comprehend the biogeochemical and ecological effects of virus (Bratbak et al., 1992; Fuhrman 1999). Both are of great importance for understanding the carbon flow in the microbial food web; both topics, however, were beyond the scope of the present study to investigate in detail, but are included to shallow extend.

Even though bacteria, small phytoplankton, and heterotrophic protists are trophically closely linked, most studies focus on one or two of the planktonic groups. To our knowledge, the current study is one of a few (Seuthe et al., 2011 and Christaki et al., 2001) that include all functional groups of microbial plankton. The lack of a more holistic approach in studies of marine microbial ecology has diminished the understanding of the grazing of heterotrophic protists, especially the nano-sized. It has long been assumed that heterotrophic nanoflagellates feed on pico-phytoplankton (Azam et al., 1983), still recent studies on the grazing of heterotrophic nanoflagellates focus on quantifying bacterivory, and only speculate about the portion of carbon taken up via pico-phytoplankton (Tanaka 1997; Iriarte et al., 2008; Vaqué et al., 2008).

In the past, there has been a strong focus on the dynamics and fate of the spring bloom in temperate and arctic ecosystems, because the new production of larger phytoplankton in this period has a strong link to mesozooplankton and fish production (Sverdrup 1953; Steele 1974; Braarud and Nygaard 1978). Spring blooms are limited in time and space, and dominated by larger phytoplankton, e.g. diatoms, from which a large fraction sinks out, contributing to the biological pump (Billett et al., 1983).

What may help resolve Steel's problem is to shift the focus from the spring bloom onto the fate of the primary production occurring the rest of the year, which is dominated by both smaller phytoplankton and smaller grazers with higher turn over rates. During the past 40 years, it has become increasingly obvious that, despite their small size, heterotrophic protists play a key role in the carbon flux in marine food webs. Since the focus has long been on the spring bloom in the northern ecosystems, during which MZP often dominate, the key role of heterotrophic protists as grazers has been overlooked, even though they are more active all year around and play an important role in structuring pelagic ecosystems (Sherr and Sherr 2002) and even though it is well documented that the grazing of μZP exceeds that of MZP in contrasting marine systems (Levinsen and Nielsen 2002; Calbet 2008).

Similarly pico- to nano phytoplankton, have been overlooked in the northern ecosystems, since they make up a relatively small part of the diatom dominated spring bloom period. In addition, they have long been considered restrained to oligotrophic tropical waters, given their high affinity for nutrients (Tremblay et al., 2009). Small primary pro-

ducers, however, appear to be important even in Temperate and Polar Regions: Joint et al. (1993) found that <5 μm phytoplankton accounted for more than 65 % of the primary production at 60°N in pre- and post bloom conditions. Small phytoplankton cells can also be found in high numbers in the ice-covered Arctic Ocean (Vaqué et al., 2008; Seuthe et al., 2011). Estimates show that pico-phytoplankton contribute to 39 % of global planktonic primary production and constitute 24 % of the standing biomass, the discrepancy between the two parameters being caused by the high turnover rate of pico-phytoplankton (Agawin et al., 2000). It has been speculated that the warming of the northern Atlantic may be causing pico-phytoplankton to become increasingly dominant (Li et al., 2009). If so, their seasonal distribution and the fate of the primary production that they contribute become increasingly important to understand.

The North Atlantic is a highly productive area and an important sink for atmospheric carbon dioxide (Robertson et al., 1993). A major portion of the annual drawdown of carbon dioxide is via the biological pump and results largely from the spring bloom (Billett et al., 1983), which is part of the reason why considerable effort has been put into increasing the understanding of the controls on the development of the bloom i.e. the North Atlantic Bloom Experiment. Efforts, however, have largely focused on the Atlantic below 50°N, even though the carbon sink of the Subpolar to Polar region is strong.

In the current study, we focus on the transition-period from winter to spring, i.e. the pre-bloom, of the Subpolar North Atlantic. We describe the succession of heterotrophic protists and their prey, and with a more experimental approach, present estimates of the importance of the protist grazing, in this understudied period of the seasonal cycle.

3 Materials and methods

3.1 Sampling

The study was conducted from March 25th to April 29th 2012 during a cruise aboard the RV Meteor (cruise no. 87), University of Hamburg. The study covered 3 stations located in the region defined as the Sub-polar North Atlantic by Longhurst (1995). Sampling was done in different hydrographic regimes: 2 deep basin stations on either side of the Greenland-Scotland Ridge and one shallow station on the Shetland Shelf (fig. 1). To describe the seasonal succession, each location was visited repeatedly with ca. 10 days intervals during the cruise.

Vertical profiles of temperature, salinity, PAR and fluorescence were obtained using a CTD Sea Bird (SBE 9 plus). Fluorescence was converted into chlorophyll *a* (Chl *a*) by calibrating fluorescence at each visit with measured Chl *a*. The euphotic layer was estimated from direct PAR measurements and not % of surface PAR, as surface PAR so far was not available. Based on the water column structure, 5 to 14 depths were sampled both within and below the mixed layer and near the bottom, using a rosette of 10 L Niskin bottles attached to the CTD. Samples were collected to provide data on Chl *a* and the abundance of virus like particles (thereafter referred to as virus), heterotrophic prokaryotes (bacteria), small phytoplankton, unidentified heterotrophic nanoflagellates (HNF), heterotrophic dinoflagellates and ciliates.

Sampling was done in triplicates within intervals of 6-24 h, to capture the variation during station time. Due to the analysis time of samples, the sampling of bacteria, virus, small phytoplankton, and total Chl *a* was about twice as frequent as the sampling of more time consuming HNF, microzooplankton and fractionated Chl *a*. Mixed layer depths (MLD) were identified as a decrease of 0.2 °C from surface (10 m) temperatures (de Boyer Montégutet et al., 2004), found to be the most appropriate in high latitude regions of deep convection (MLD are given in table 2, 3, 4). The weather conditions were generally windy and evidently caused mixing in addition to the convection. The Icelandic Basin was most stormy, where winds reached 8 Bft during the 2nd visit. By the 3rd visit there had just been 2 days of storm (12 Bft with gusts of 14 Bft), and sampling was completed during 7 Bft and 3-4 m waves.

Nutrients

Nitrite and nitrate (N), phosphate (P) and Silicate (Si) were measured throughout the water column directly after sampling using a Skalar Sanplus segmented-flow autoanalyser. The methods used are that of Wood et al., (1967) for the determination of nitrate/nitrite, that of Murphy and Riley (1962) for phosphate and that of Koroleff (1983) for the determination of silicate. Quality assessment of the analysis showed that the variations observed throughout the cruise were within the analytical error of the method (M. Esposito, pers. comm.).

Chlorophyll *a*

Chl *a* was determined from triplicate water samples of 100-1000 ml and size fractionated on Whatman GF/F filters with 0.7 μm pore-size, 10 μm mesh filters and 50 μm mesh filters. Filters were extracted in 96 % ethanol for 12-24 h (Jespersen and Christoffersen 1987). Chl *a* concentration was measured before and after addition of acid (1 M HCl) on a TD-700 Turner fluorometer calibrated against a Chl *a* standard.

3.1.1 Flow cytometric enumeration

Bacteria, viruses, small phytoplankton and HNF were enumerated using a FACS Calibur (Beckton Dickinson) flow cytometer, with an air-cooled argon ion laser (488 nm, 15 mW) as the fluorescence excitation light source. Flow cytometric data was analysed using CellQuest software (Becton Dickinson, Oxford, UK). The cell numbers were calculated from the instrument flow rate based on volumetric measurements ca. every 4 h.

Bacteria and viruses

Samples for bacteria and viruses were fixed with glutaraldehyde (final conc. 0.5%) for 30 min in the dark at 4 °C and thereafter flash-frozen in liquid nitrogen and stored in - 80 °C until further analysis performed within 4 months. Samples were thawed and appropriate dilutions (5- and 10-fold) of fixed samples were prepared in 0.2 μm filtered TE buffer (Tris 10mM, EDTA 1mM, pH 8) and stained with a green fluorescent nucleic-acid dye (SYBR Green I, Molecular Probes Inc., Eugene, OR) and kept for 10 min at + 80 °C water bath to provide optimal staining of virus (Brussaard 2004). As reference, yellow-green fluorescent beads of 2 μm (FluoSpheres® Carboxylate-Modified Microspheres, UK) were added to all samples in 20 x 10^6 fold dilution of stock. Samples

were analysed for 1 min at a flow rate of ca. 30 µl min^{-1}. Determination of the prokaryote population was based on scatter plot observations of the light side-scatter signal vs. the green fluorescence signal (FL-1) of SYBR Green I. Settings were FSC = E02; FL-1 = 520; FL-2 = 500; FL-3 = 700; Threshold = 20.

Small phytoplankton

Samples were preserved as bacteria and viruses, and analysed directly after thawing for 5 min at a flow rate of 60-70 µl min^{-1}. Settings were FSC = E02; FL-1 = 400; FL-2 = 550; FL-3 = 450; Threshold = 52. Gates were made for pico eukaryotes, pico prokaryotes and nano phytoplankton, and were discriminated on the basis of their side scatter, Chl *a* and phycoerythrin fluorescence as in Bratbak et al., (2011). In our samples the pico prokaryotes were entirely dominated by the genus *Synechococcus* sp., in accordance with Cottrell et al., (2008), who found the abundance of *Prochlorococcus* sp. to be insignificant in the Icelandic Basin.

Heterotrophic nanoflagellates

Samples were fixed for 2 h with glutaraldehyde (final conc. 0.43 %) at 4 °C in the dark, thereafter receiving same handling as bacteria. Samples were stained with SYBR Green I for 2-4 h in the dark at 4 °C and 0.5 µm yellow-green fluorescent beads were added. HNF were discriminated from phototrophic nanoflagellates in bivariate plots of the SYBR green fluorescence (FL-3) vs. red fluorescence of Chl *a* (FL-3). Settings were FSC = E02; FL-1 = 350; FL-2 = 400; FL-3 = 430; Threshold = 20 (SSC-H). With minor modifications the protocol follows that of Zubkov et al. (2007).

30 corresponding samples were taken for epifluorescence microscopy for size measurements of HNF, to complement the flow cytometric counts. These samples were fixed with glutaraldehyde (final conc. = 1 %) for 15 min and then kept at – 80 °C. A 10 ml sample was filtered through black polycarbonate filters (pore size 0.8 µm), stained with 4,6-diamidino-2-phenylin- dole dihydrochloride (DAPI) DNA-specific dye (Porter and Feig, 1980), and measured under a UV-microscope with x1000 magnification (see example supp. 6). To ensure the measured cells were heterotrophic, each cell was crosschecked for red auto-fluorescence.

3.1.2 Microzooplankton

Abundance, biomass and taxonomic composition of μZP were determined from 3 or 5 depths pr. profile by gently siphoning 500 ml subsamples into brown glass bottles. Samples were fixed in acetic Lugol's solution (final conc. of 4 %) and stored in the dark at room temperature until analysis, which was performed within 8 months. The most dilute samples were allowed to settle 48 h in a 500 ml graduated cylinder and the upper 400 ml of the sample was gently siphoned out of the cylinder in order to up-concentrate the sample. 50 ml subsamples were allowed to settle for at least 18 h in Hydrobios sedimentation chambers. All or a minimum of 400 cells were counted using an inverted microscope with x200 magnification (see example supp. 6). Cells were categorized as dinoflagellates or ciliates and divided into size classes using their length (<20 μm, 20-35 μm, 35-60 μm, >60 μm) and most abundant genera and species. Cell volumes were calculated using appropriate geometric forms and converted to cell carbon using standard volume to carbon conversion factors (table 1). To compensate for shrinkage of cell volume due to Lugol's preservation, cell volumes were increased by a factor of 1.3 (Stoecker et al., 1994). Equivalent spherical diameter (ESD) of the μZP is related by: $\pi/6 \times \mathrm{ESD}^3$ = cell volume, used in the later for biomass estimations.

3.1.3 Biomass estimations

Biomass for each of the functional groups was calculated using published conversion factors (table 1) best representing our samples, e.g. those estimated from the northern North Atlantic if possible. The same carbon to Chl *a* conversion factor of 21 (Bratbak et al., 2011) was used for all calculations at the three stations despite different phytoplankton composition and sampling depth. Integration by the trapezoid rule was applied down to the base of the MLD for the deep stations (table 2), and down to 100 m at the fully mixed Shetland Shelf station. The calculated MLD is the end point of integration, but when samples were not available this exact depth, a curve fit was made between the two neighbouring samples and the resulting curve equation used to estimate the value of the base of the mixed layer. The integrated values were converted to mg C m^{-3} to better enable comparison.

Table 1: The chosen carbon conversion factors and references for different organisms and Chl *a*.

Group	**Carbon conversion factor**	**Reference**
Chl *a*	21 g C pr. g Chl *a*	Bratbak et al., 2011
Nano phyto.	3530 fg C cell^{-1}	Tarran et al., 2006
Pico eukaryotes	440 fg cell^{-1}	Terran et al., 2006
Synechococcus sp.	110 fg C cell^{-1}	Tarran et al., 2001
Virus	0.08 fg C virus^{-1}	Jacquet et al., 2002 according to Bratbak et al., 1992
Bacteria	20 fg C cell^{-1}	Lee and Fuhrman 1987
HNF	220 fg C μm^{-3}	Børsheim and Bratbak 1987
Aloricate ciliates	Log (pg C cell^{-1}) = -0.639 + 0.984 Log (V)	Putt and Stoecker 1989, modified by Menden-Deuer and Lessard 2000
Loricate ciliates	Log (pg C cell^{-1}) = -0.168 + 0.841 Log (V)	Verity and Langdon 1984, Menden-Deuer and Lessard 2000
Dinoflagellates	Log (pg C cell^{-1}) = -0.353 + 0.864 Log (V)	Menden-Deuer and Lessard 2000

3.2 Experimental setup

Three shipboard microcosm experiments were conducted sequentially from the end of March to April 2012 for the Icelandic Basin station. Water was collected from the photic zone at 30 % PAR (ca. 30 m depth) using 10 L Niskin bottles and water was gently siphoned into dark carboys. Before setup of the experiments all bottles and carboys were acid washed, left standing with seawater for 24 h and rinsed in milliQ water. For the microcosm experiments, 50 L of the collected water was manipulated by screening seawater through different sizes of filters to minimize the number of multicellular microzooplankton and mesozooplankton (>50 μm), microzooplankton (>10 μm) and nanoflagellates (>0.8 μm). The different seawater fractions were prepared by gently screening the water through either a 50 μm or a 10 μm mesh filter by reversed filtration, or by screening using a pump though a 0.8 μm polycarbonate filter placed over a wetted GF/F filter. Water from each treatment was gently transferred into triplicate 1.6 L transparent polycarbonate bottles using silicone tubing. Initial abundance of organisms in each treatment of experiment is given in table 5. Another 50 L of seawater was filtered through a 0.2 μm sterile Polycarp filter and thereafter stored in the dark at 1 °C for later addition to the microcosm experiments (max 10 days of storage). Control samples of the stored water showed no noteworthy increase in the bacterial abundance during the period.

The experimental bottles were incubated in a 1000 L PVC tank with flow-through water running from a 5 m depth at a temperature near to in situ (5-13 °C in microcosm 1 and 7-11 °C in microcosm 2 and 3). To ensure light conditions similar to where the water was collected, experimental bottles were placed in dark nylon bags, which reduced to 30 % light intensity. The bottles were kept in motion by the vessel's movements and stirred daily by hand.

Every other day, 260 ml subsamples for counting viruses, bacteria, pico- and nanophytoplankton, HNF, μZP, and for measuring fractionated Chl *a*, and nutrients (N, P, Si) were taken and analysed by methods as explained above. After each sampling event, bottles were refilled by adding appropriate volume of the stored 0.2 μm filtered seawater. The experiments were terminated after 10 days.

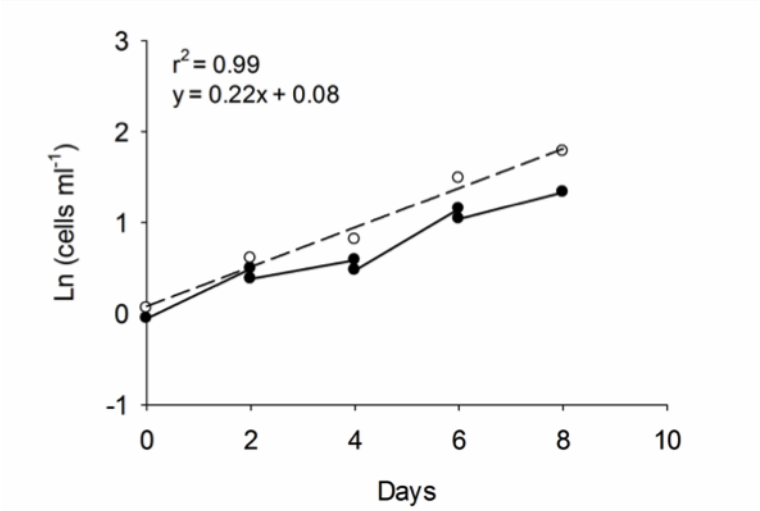

Figure 1: Example of growth calculation from Microcosm 2, number of ciliates in <50 µm treatment. Data points shows realized cell concentrations before and after dilution (black dots), the calculated growth (black lines) and estimated cumulated cell concentrations (white dots) of total number of ciliates. A linear regression has been fitted to the cumulated cell concentrations from day 0-8 (dotted line). The estimated growth rate (µ, d^{-1}) is given as the slope of the regression.

3.2.1 Growth and grazing rates

Nat growth rates (µ, d^{-1}) were calculated as the increase in cell concentration according to:

$$\mu(d^{-1}) = \frac{lnN - lnN_0}{t_1 - t_0}, \tag{1}$$

where N_0 and N_1 are number of cells at time t_0 and t_1, respectively and t is the difference in time (d) between samples taken at t_0 and t_0. Dilution of the cultures was taken into account by estimating cumulated cell concentrations, N_{cum} to the time t:

$$N_{cum}(cells\ ml^{-1}) = N_{t-1} \cdot e^{\mu(t_1 - t_0)}, \tag{2}$$

where N_{t-1} is the number after dilution, calculated as $N_{measured} - \frac{vol.removed}{total.vol} \cdot N_{measured}$ and µ is the growth rate from N_{t-1} to the undiluted value of N_t.

Average net growth rates (n=3) presented in the later were calculated as linear increase in ln (N_{cum}) during the exponential growth face of the incubation. An example of a growth rate calculation is illustrated in fig. 1

Clearance rates (Cl, ml cell^{-1} d^{-1}) and ingestion rates (I, µg C cell^{-1} d^{-1}) of heterotrophic protists were calculated after a modification of Frost (1972) and Kiørboe et al., (1982), when prey growth rates differed significantly between the size treatments (i.e. between >50 µm and >10 µm treatments or between >10 µm and >0.8 µm treatments) (t-test, $p < 0.05$).

$$Cl = 24 \cdot (\frac{V}{n \cdot t}) \cdot ln\Big(\frac{C_1^* \cdot C_2}{C_1 \cdot C_2^*}\Big), \tag{3}$$

Where V = volume of experimental bottles (ml), n = difference in number of heterotrophic protists between two treatments, $t = t_2 - t_1$ (h), C_1 and C_2 = prey concentration (cells ml^{-1}) in the smallest size treatment (> 0.8 µm or > 10 µm at the start (t_1) and the end (t_2) of the experiment, respectively C_1^* and C_2^* = prey concentration (cells ml^{-1}) in the larger size treatments (>10 µm or >50 µm) at (t_1) and (t_2), respectively.

$$I = \left(\frac{C_2^* - C_1^*}{ln\Big(\frac{C_2^*}{C_1^*}\Big)}\right) \cdot C_{prey} \cdot Cl \tag{4}$$

Where C_1^* and C_2^* = prey concentration (cells ml^{-1}) in the larger size treatment at (t_1) and (t_2), respectively, C_{prey} = prey carbon content (µg C cell-1) and Cl = clearance rate (ml cell^{-1} d^{-1}) from Eq. 3.

4 Results

4.1 Hydrography

The study was conducted at three hydrographically different locations in the Subpolar Atlantic. The Faroe current and Shetland current are the dominant surface currents of the area, transporting warm saline Atlantic Water (potential temp. of 5-10.5 °C, salinity 35-35.05) into the Nordic Sea and Arctic Ocean (fig. 2)(Hansen and Østerhus 2000).

In the Polar Region, cooling leads to the formation of Deep Water (potential temp. <0.5°C, salinity 34.88-34.93), which fills up the bottom of the Norwegian basin and forms bottom currents (somewhat slower than the surface currents), and balancing the inflow of Atlantic Water. When Deep Water crosses over the Greenland-Scotland ridge it is called Overflow Water (Hansen and Østerhus 2000).

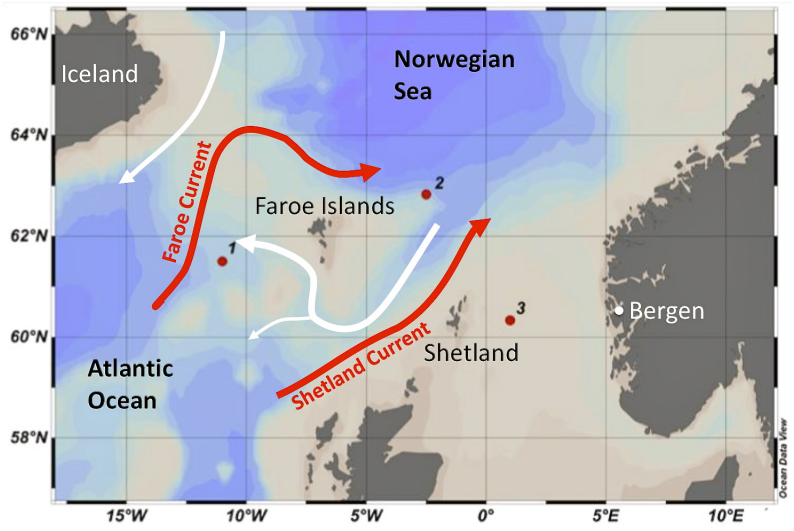

Figure 2: Study area in the North Atlantic. (1) marks the 1350 m deep station in the Icelandic Basin (61.5°N, 11°W). (2) marks the 1300 m deep station in the Norwegian Basin (62.8°N, 2.5°W) and (3) marks the 160 m deep station on the Shetland Shelf (60.3°N, 1°E). Arrows illustrating the dominating currents, red = Atlantic Water transported at the surface, white = Deep- and Overflow Water from the Arctic. Map created using ODW, currents are drawn based on Hansen and Østerhus (2000).

From T-S diagrams all three stations appeared to be characterized by stable water masses throughout the investigated period. The only variations occurred in the Icelandic Basin at 1000-1300 m depth due to intruding intermediate water masses (fig. 3). The Iceland Basin consisted mostly of Atlantic Water reaching $>$ 1000 m, the rest being intermediate water masses. Polar Overflow Water was observed only at the deepest 100 m of the Iceland Basin. At the Norwegian Basin station the Atlantic Water was restrained to the upper 100-200 m of the water column and the major part (400-1300 m) consisted of Deep Water. The Shetland Shelf station was characterized by a very uniform water mass of Atlantic Water (fig. 3).

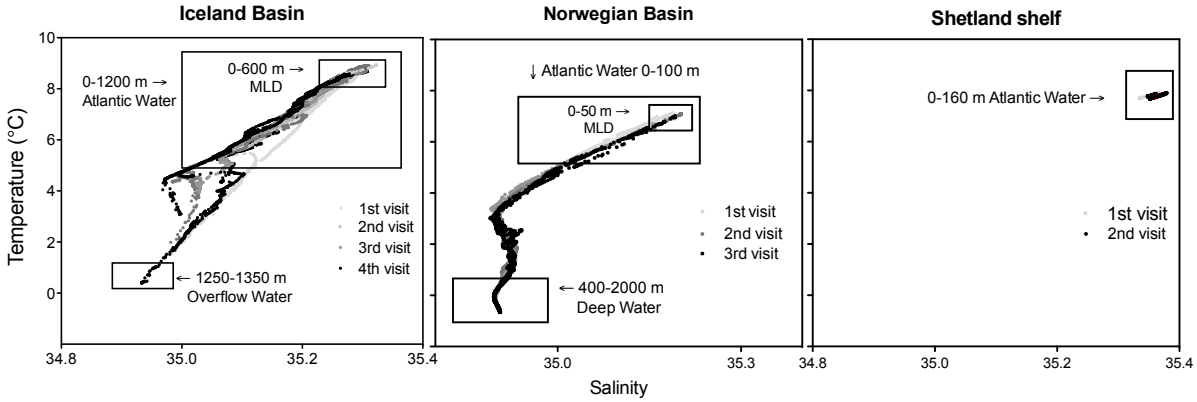

Figure 3: T-S diagrams from all measured profiles at each station. Water masses are defined according to Blindheim and Østerhus (2005). Boxes roughly indicate the depths of the dominant water masses - the rest being intermediate water. Also boxes mark the upper mixed layer water.

Iceland basin

The station located in the Iceland basin was visited four times from the end of March to the end of April; 1^{st} visit (26-28.03), 2^{nd} visit (7-10.04), 3^{rd} visit (18-21.04), 4^{th} visit (27-29.04). At the first visit MLD reached 600 m depth, but by the end on the investigated period the MLD reduced to 344 m (table 2). The euphotic layer extended down to approx. 100 m throughout the investigated period and Chl *a* was mixed well below this layer. Temperature within the MLD ranged between 7.9-8.9 °C and the salinity between 35.2-35 (fig.4). At the first visit maximum Chl *a* concentration was 0.3 µg l^{-1}. The rest of the investigated period maximum Chl *a* concentration ranged between 1.4-2.1 µg l^{-1} and was measured at 15 - 71 m depth. Below the mixed layer, at 720-1200 m distinct low oxygen concentrations were observed; 240 µmol kg^{-1} in contrast to 272 µmol O_2 kg^{-1} in the surrounding water, which is a permanent feature of the area observed in

online datasets like Glodap, WOCE and Carina (A. Rullyanto, pers. comm.).

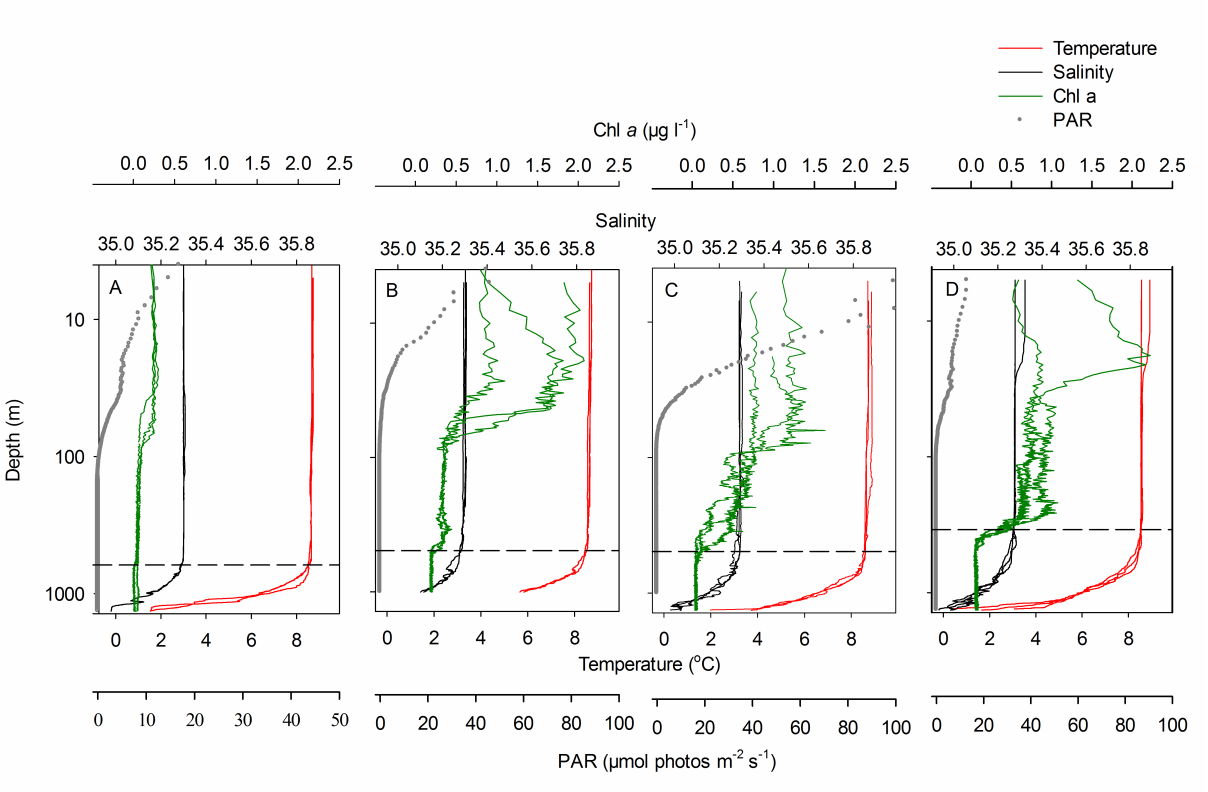

Figure 4: Vertical profiles of temperature, salinity, Chl a and PAR in the Icelandic Basin. A: 1^{st} visit (26-28.03), B: 2^{nd} visit (7-10.04), C: 3^{rd} visit (18-21.04), D: 4th visit (27/4-29/4). Horizontal dashed line indicates the depth of the mixed layer.

Norwegian basin

The station located in the Norwegian Basin was visited three times, from end-March to end-April; 1^{st} visit (30-31.03), 2^{nd} visit (13-14.04), 3^{rd} visit (22-25.04). The defined MLD of the Norwegian Basin was relatively shallow (around 50 m) at all visits (Table 3). However deeper stratification was evident due to the different properties of the upper 100-200 m Atlantic Water and under-laying polar Deep Water. The euphotic layer extended down to approx. 100 m at all times and maximum Chl *a* was found within this zone. At the first visit the Chl *a* maximum was 0.5 µg l^{-1}. The rest of the investigated period maximum Chl *a* concentration ranged between 0.8-1.3 µg l^{-1} and was measured at 5-10 m depth. Within the period of sampling a steep salinity and temperature gradients were found in the upper 200 m, caused by the difference of the upper AW and intermediate water masses. Temperature was 7.1 °C in the upper mixed 50 m and towards the bottom decreased to <0 °C (fig. 5). The daily variation of Chl *a* was strong at the deep stations and could exceed the variation between visits.

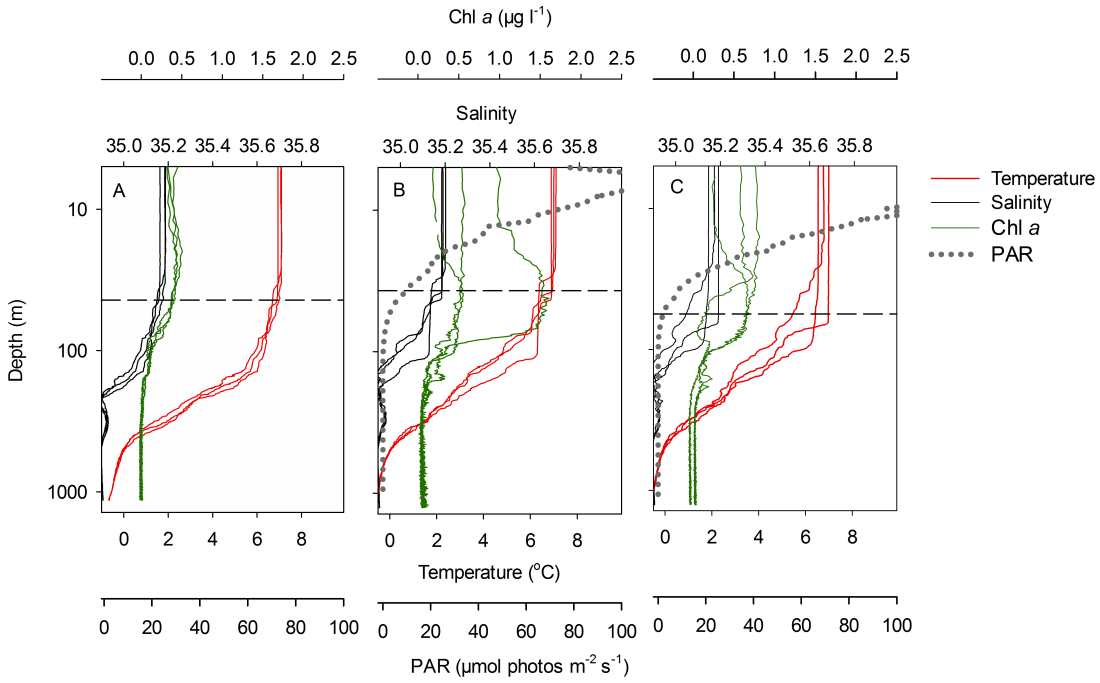

Figure 5: Vertical profiles of temperature, salinity, Chl *a* and PAR in the Norwegian Basin. A: 1^{st} visit (30-31.03), B: 2^{nd} visit (13-14.04), C: 3^{rd} visit (22-25.04). Horizontal dashed line indicates the depth of the mixed layer.

Shetland Shelf

The station at the Shetland shelf was visited twice; 1^{st} visit (02.04), 2^{nd} visit (15-16.04). The station was only 160 m deep resulting in a fully mixed water column, caused by both winter convection and tidal mixing (Shaples et al., 2006). Thus, temperature and salinity varied only slightly: 7.7-7.9 °C and 35.3-35.4 respectively (fig.6). The euphotic layer extended down to ca. 60 m at the 1^{st} visit and decreased to 40 m by the 2nd visit. Chl *a* was distributed evenly throughout the water column, maximum measured Chl *a* ranging between 0.6-3.4 µg l^{-1} at 10-75 m depth and profiles were spiky (fig. 6), possibly indicating presence of larger phytoplankton or aggregates (Briggs et al., 2011).

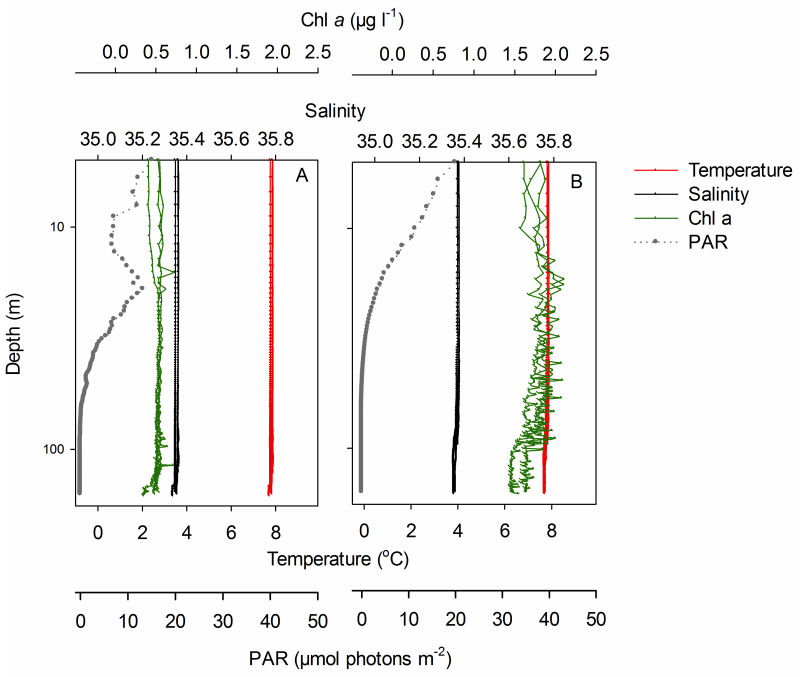

Figure 6: Vertical profiles of temperature, salinity, Chl *a* and PAR from the Shetland Shelf. A: 1^{st} visit (02.04), B: 2^{nd} visit (15-16.04).

Nutrients

High concentrations of NO_2^{-1}+NO_3^{-1}, PO_4^{-1} and Si (hereafter written as N, P, Si) were found at all stations during the investigated period. For most nutrients there was a statistically significant decrease in the upper mixed layer during the period (see fig. 7 and supp. 1). Si concentrations were lower at the Iceland Basin (avg. 4.5 µM) and gradually decreased through the period, while at the Norwegian basin Si did not decrease (avg. 5.5 µM), corresponding well to the relative presence of diatoms at the respective stations. At the deep stations, nutrients increased towards the bottom with a nutricline at about 200 m at the Norwegian Basin, while in the Iceland Basin a high nutrient zone was observed in the depths of the low oxygen zone (700-1200 m) with the highest observed nutrients in the survey (N = 15.3 µM, P = 1 µM, Si = 7.7 µM). As these follow the Redfield ratio, it is likely to assume that organic material has been remineralized and may also explain the low oxygen. Close to the bottom of the Iceland Basin nutrient concentration decreased, caused by the low nutrient content of the Overflow Water (Stefánsson 1968). At the Shetland Shelf, nutrient concentration were distinctly lower (N = 9.5 µM, P = 0.6 µM, Si = 2.8 µM) than at the two deep stations, and by the last visit Si concentrations had been depleted to 1.7 µM (fig.7 and supp 1) due to the developing diatom bloom. See averaged nutrient concentrations within and below MLD in supp. 1, and for better comparison of changes of the respective nutrients see profiles supp. 2.

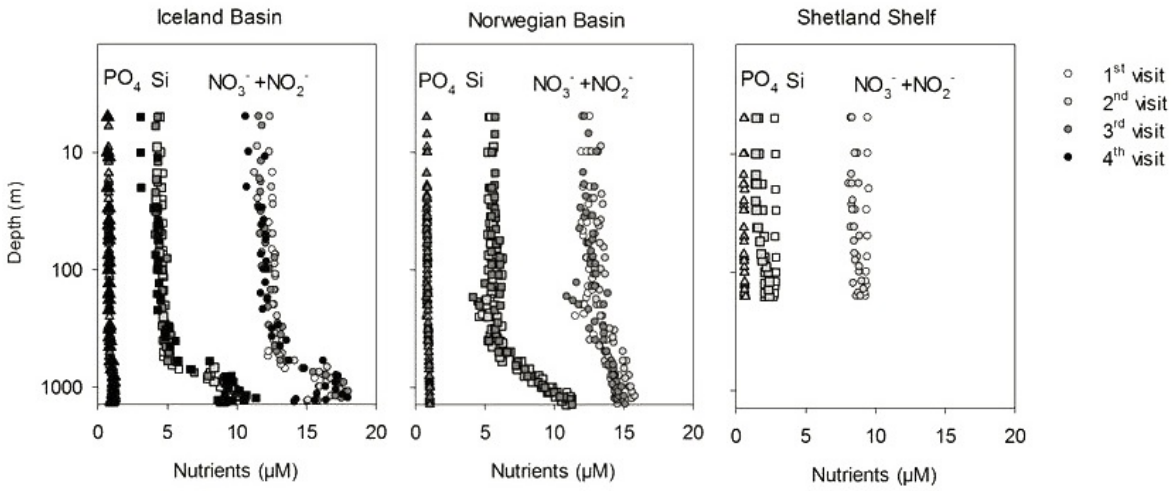

Figure 7: Profiles of measured nutrients at the three stations through the period (log-scale). △ = PO_4^-, □ = Si and ○ = NO_3^- + NO_2^-.

Dissolved organic matter

DOC was measured during the study throughout the water column. The deep sea (3000 m) of the North Atlantic contain a higher concentration of DOC any deep ocean areas in the world (Hansell et al., 2009) around 46 µmol kg^{-1}, this was in accordance with our deep measurements of DOC, which at 1300 m was around 50 µmol kg^{-1}, with decreasing concentration towards the bottom (supp. 1 and 7). The DOC in the upper mixed layer increased significantly from the first to the second visit at the Iceland Basin (t-test, P = 0.02) most likely caused by the concurrent high increase in phytoplankton biomass, while the rest of the period DOC did not change (one-way anova, P = 0.53). Similar increase was observed on the Shetland Shelf, while DOC did not change at the Norwegian Basin.

4.2 Succession of autotrophic biomass

For all stations the averaged phytoplankton biomass was lowest at the 1^{st} visit and more than doubled within 10-14 days (table 2, 3, 4). While the phytoplankton biomass increased through the entire period in the Icelandic Basin and Shetland Shelf, there was no increase from 2^{nd} to 3^{rd} visit in the Norwegian Basin. Based on flow cytometer counts, observations from lugol preserved samples, and fractionated Chl *a*, we saw how phytoplankton composition differed between the stations and changed over time.

Larger phytoplankton

The Norwegian basin was strongly dominated by phytoplankton <10 µm throughout the study period. Pico phytoplankton dominated in the beginning, whereas nano-sized phytoplankton, mainly of the class *Cryptophyceae* spp., became more important in the end of the period, were diatoms remained absent.

Phytoplankton <10 µm including *Cryptophyceae* spp. only dominated the Icelandic Basin at the 1^{st} visit. By the 2^{nd} visit high abundance of *Chaetoceros* spp. (up to 200 cells ml^{-1}) was observed and a few *Leptocylindricus* spp. This was reflected in the Chl *a*, as the >50 µm fraction came to comprise about 50 % of the phytoplankton biomass. By the last two visits *Pseudo-nitzschia* spp. became more dominant, but overall total diatom abundance decreased. The succession at the Shetland Shelf was similar to the Icelandic Basin with increasing importance of >50 µm Chl *a* and high abundance of diatoms, mainly *Thalassiosira* spp. and *Ditylum brightwelli* at the 2^{nd} visit.

Pico- and nano phytoplankton

In the beginning of the sampling period, pico eukaryotes dominated in number over *Synechococcus* spp. and nano- phytoplankton (table 2, 3, 4), but by the end of the sampling period, the pico eukaryotes decreased considerably in numbers at all stations. See organism profiles supp. 3.. The small phytoplankton were detected throughout the mixed layer at all stations (see organism profiles supp. 3) and maximum abundance of the small phytoplankton was in 24 out of 27 cases found in sub-surface samples (below 5 m). Coccolithophores were counted in polarizing light microscopy and showed low abundance (<12 cells ml^{-1}) at all times and all stations (C. Daniels, unpublished).

The Norwegian Basin had the highest concentrations of small phytoplankton, about twice that of the Iceland Basin and 3 times that of the Shetland Shelf. Pico eukaryotes, *Synechococcus* spp. and nano-phytoplankton ranged from 6-11.6 $\times$ 10^3, 2.3-4.7 $\times$ 10^3 and 0.4-1.3 $\times$ 10^3 cells ml^{-1} averaged over the mixed layer, respectively. While pico eukaryotes decreased in numbers, nano-phytoplankton increased significantly through the period (one way anova, P = 0.0215). At the Icelandic Basin, pico eukaryotes, *Synechococcus* spp., and nano-phytoplankton ranged between 0.8-5 x 10^3 cells ml^{-1}, 0.7-1.6 x 10^3 cells ml^{-1}, and 0.2-0.5 x 10^3 cells ml^{-1} respectively. The Shetland Shelf had the lowest concentration of small phytoplankton, pico eukaryotes, *Synechococcus* spp., and nano-phytoplankton, ranging between 0.4-1.5 $\times$ 10^3, 0.3-0.6 $\times$ 10^3, and 0.2-0.3 $\times$ 10^3 cells ml^{-1}, respectively (fig.8).

The summed biomass (expressed as carbon, table 1) of pico- and nano-phytoplankton was correlated to the Chl *a* <10 μm fraction, however correlations were rarely strong. Significant correlations are shown in table 2, 3, 4 and all plots can be found in supp. 4. The averaged value of the slopes of significant correlations resulted in a low carbon conversion factor of 9.4 ± 3.7, n = 5 for the small phytoplankton. The low Chl *a* conversion factor most likely is caused by a discrepancy between the <10 μm Chl *a* and the pico- and nano phytoplankton counted on the flow cytometer, as a fragment of the nano phytoplanton are >10μm, or a discrepancy in the applied carbon conversion (table 1).

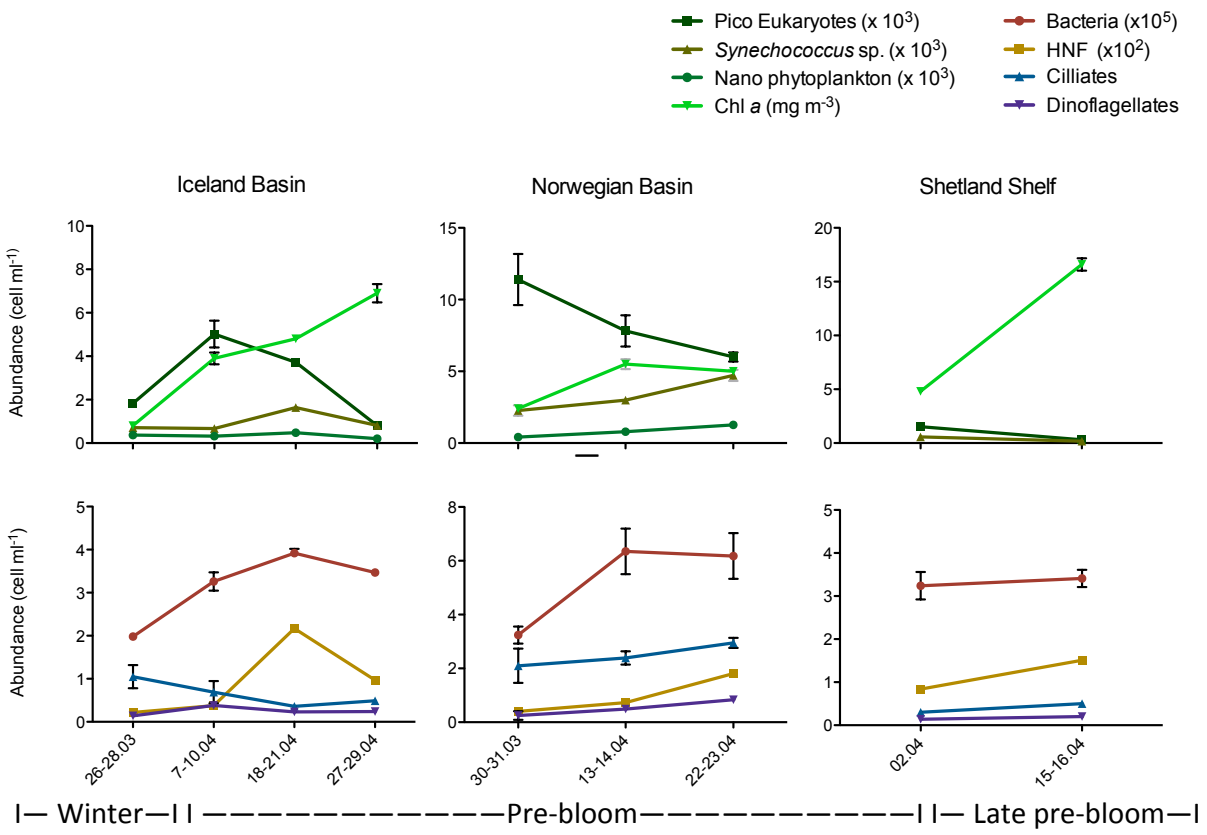

Figure 8: The succession of autotrophic and heterotrophic protists, vales presented as mean abundance ± SD within the upper mixed layer over time (values also presented in table 2, 3, 4). Note different axis. Lower dashed line indicates roughly the seasonal state of the system, which varied between stations.

Table 2: Concentration of Chl *a* and abundance of small phytoplankton (10^3 x cells ml^{-1}), bacteria (10^5 x cells ml^{-1} heterotrophic protist (cells ml^{-1}) at the Iceland Basin. Values given as mean ± SD, n, (min, max) within the mixed layer, as well as averaged size of µZP. Procentage (%) of Chl *a* fractions and the correlation of biomasss (C) of pico- and nanophytoplankton to the >10µm Chl *a* fraction. V:B calculated for both within and below MLD and the ratio of heterotrophic biomass (HB) to autotrophic biomass (AutoB).

Iceland Basin	**1^{st} visit**	**2^{nd} visit**	**3^{rd} visit**	**4^{th} visit**
MLD	618 m	493 m	492 m	344 m
Chl *a* (µg l^{-1})	0.1 ± 0, n = 21 (0, 0.3)	0.4 ± 0.1,n = 20 (0, 2)	0.5 ± 0.1, n = 22 (0, 1.4)	0.7 ± 0.2, n = 20 (0.1, 2)
Chl *a*>10µm(%)	13.1 ± 5.2	81.3 ± 14.1	53.7 ± 14.6	62.2 ± 12.6
Chl *a*>50µm(%)	4.7 ± 2.8	55.5 ± 31.1	45.1 ± 19.8	49.2 ± 11.3
PicoE.	1.8 ± 0.4, n = 16 (0.3, 4.2)	5.0 ± 2.3,n = 14 (0.7, 8.9)	3.7 ± 0.6, n = 16 (1.1, 5.7)	0.8 ± 0.3,n = 12 (0.2, 1.4)
Synec.	0.7 ± 0.1, n = 16 (0.3, 1.4)	0.7 ± 0.1,n = 14 (0.3, 0.9)	1.6 ± 0.2, n = 16 (0.4, 2.5)	0.8 ± 0.1,n = 12 (0.2, 1.2)
Nano phyto.	0.4 ± 0.2, n = 16 (0.1, 1.2)	0.3 ± 0.2,n = 14 (0.1, 0.7)	0.5 ± 0, n = 16 (0.2, 0.8)	0.2 ± 0.1,n = 12 (0, 0.4)
C:Chl *a*<10	15.8 ± 3 (P<0.05)	-	6.3 ± 1 (P<0.05)	-
Bacteria	2 ± 0.2, n = 16 (0.8, 2.8)	3.3 ± 0.9,n = 16 (1.7, 5.5)	3.9 ± 0.4, n = 16 (2.4, 4.7)	3.5 ± 0.1,n = 12 (2.4, 4.6)
V:B in MLD	8.2 ± 0.6, n = 16	6.1 ± 1.3, n =16	2.9 ± 0.6, n = 15	2.6 ± 0.3,n = 12
V:B below MLD	4.4 ± 2.0, n = 6	6.3 ± 1.9, n = 5	7.3 ± 2.1, n = 6	4.7 ± 0.9, n = 9
HB:AutoB	2.9 ± 0.2	0.3 ± 0.1	0.3 ± 0.03	0.1 ± 0
HNF	22.1 ± 4.5, n = 9 (14.4, 17.6)	37.8 ± 1.6, n = 10 (20, 63.1)	217 ± 22.5, n = 11 (122.2, 307.7)	97.1 ± 6.3, n = 8 (65.7, 147.7)
Ciliates	1.1 ± 0.9, n = 11 (0.1, 2.6)	0.7 ± 0.8, n =10 (0.2, 0.7)	0.4 ± 0.3, n = 10 (0.1, 1.1)	0.5 ± 0.3, n =8 (0.2, 1)
Dinoflagellates	0.1 ± 0.1, n = 11 (0, 0.4)	0.4 ± 0.2, n =10 (0.2, 0.7)	0.2 ± 0.1, n =10 (0.1, 0.4)	0.2 ± 0.1, n =8 (0.1, 0.5)
ESD, Cil (µm)	19.2 ± 2.5, n = 2414	23.3 ± 3.9, n = 1372	24.5 ± 2.7, n = 911	26.4 ± 2.2, n = 994
ESD, Dino (µm)	21.0 ± 3.6, n = 320	22.0 ± 3.1, n = 876	21.8 ±2.8, n = 550	25.7 ± 3.0, n = 474

Table 3: Concentration of Chl *a* and abundance of small phytoplankton (10^3 x cells ml^{-1}), bacteria (10^5 x cells ml^{-1} heterotrophic protist (cells ml^{-1}) at the Norwegian Basin. Values given as mean ± SD, n, (min, max) within the mixed layer, as well as averaged size of µZP. Procentage (%) of Chl *a* fractions and the correlation of biomasss (C) of pico- and nanophytoplankton to the >10µm Chl *a* fraction. V:B calculated for both within and below MLD and the ratio of heterotrophic biomass (HB) to autotrophic biomass (AutoB).

Norwegian Basin	**1^{st} visit**	**2^{nd} visit**	**3^{rd} visit**
MLD	43 m	37 m	56 m
Chl *a* (µg l^{-1})	0.2 ± 0.1, n = 17 (0, 0.5)	0.6 ± 0.2, n = 21 (0, 1.4)	0.5 ± 0.1, n = 20 (0, 0.9)
Chl *a*>10µm(%)	2.9 ± 1.4	8.3 ± 7.7	5 ± 2.3
Chl *a*>50µm(%)	0.2 ± 0.7	0.5 ± 0.3	1 ± 0.2
PicoE.	11.4 ± 4.4, n = 6 (6.3, 19.5)	7.8 ± 2.4, n = 5 (4, 10.5)	6 ± 0.8, n = 7 (4.3, 7.3)
Synec.	2.3 ± 0.9, n = 6 (0.3, 3.6)	3 ± 0.3, n = 5 (2.6,3.4)	4.7 ± 1, n = 7 (3.0,5.5)
Nano phyto.	0.4 ± 0.3, n = 6 (0, 0.8)	0.8 ± 0.1, n = 5 (0.7, 1)	1.3 ± 0.2, n = 7 (0.9,1.7)
C : Chl *a* < 10	-	5.3 ± 1.8 (P = 0.036)	10.2 ± 0.9 (P< 0.001)
Bacteria	3.2 ± 0.8, n = 6 (1.2,4.4)	6.4 ± 2.1, n = 6 (3.3,11.6)	6.2 ± 0.4, n = 7 (5.5,6.6)
V:B in MLD	4.4 ± 1.9, n = 6	3.1 ± 0.3, n = 6	2.5 ± 0.4, n = 7
V:B below MLD	6 ± 0.8	5.1 ± 1.04, n = 14	4.5 ± 0.4, n = 13
HB:AutoB	1.1 ± 0.2	1 ± 0.1	0.7 ± 0.1
HNF	40 ± 4.8, n = 3 (18.6,53.6)	73.7 ± 14.1 , n = 2 (70.5,98.7)	181.5 ± 33.1, n = 2 (148.4, 214.6)
Ciliates	2.1 ± 1.9, n =2 (0.2,4.0)	2.4 ± 0.4, n = 2 (2,2.7)	4.7 ± 1.2, n = 3 (3.7,6.3)
Dinoflagellates	0.3 ± 0.2, n = 2 (0,0.5)	0.5 ± 0.1, n = 2 (0.4,0.6)	0.5 ± 0.1, n = 3 (0.3,0.7)
ESD, Cil (µm)	20.2 ± 3.4, n = 886	19.7 ± 0.9, n = 696	23.2 ± 2.1, n = 2173
ESD, Dino (µm)	18.2 ± 1.5, n = 273	17.5 ± 2.1, n = 143	20.1 ± 4, n = 407

Table 4: Concentration of Chl *a* and abundance of small phytoplankton (10^3 x cells ml^{-1}), bacteria (10^5 x cells ml^{-1} heterotrophic protist (cells ml^{-1}) at the Shetland Shelf. Values given as mean ± SD, n, (min, max) within the mixed layer, as well as averaged size of µZP. Procentage (%) of Chl *a* fractions and the correlation of biomasss (C) of pico- and nanophytoplankton to the >10µm Chl *a* fraction. V:B calculated for both within and below MLD and the ratio of heterotrophic biomass (HB) to autotrophic biomass (AutoB). *when only one sample was avalible.

Shetland Shelf	**1^{st} visit**	**2^{nd} visit**
MLD	100 m	100 m
Chl *a* (µg l^{-1})	0.5 ± 0.04, n = 19 (0, 0.67)	1.7 ± 0.2, n = 15 (0.4, 4.8)
Chl *a*>10µm(%)	6.4 ± 1.4	55.3 ± 9.3
Chl *a*>50µm(%)	2.3 ± 0.6	42.2 ± 6.7
PicoE	1.5 ± 0.6, n = 13 (0.3, 2.5)	0.4 ± 0.1, n = 14 (0.06, 0.67)
Synec.	0.3 ± 0.1, n = 13 (0.1, 0.4)	0.6 ± 0.2, n = 14 (0.2, 1.0)
Nano phyto.	0.3 ± 0.2, n = 13 (0.1, 0.8)	0.2 ± 0.04, n = 14 (0.1, 0.4)
C : Chl *a* < 10	9.3 ± 3.9 (P = 0.041)	-0.2 ± 0.4 (P = 0.62)
Bacteria	3.4 ± 0.7, n = 13 (2.2, 8.8)	4.8 ± 0.4, n = 14 (3.8, 6.8)
V:B in MLD	4.7 ± 0.9, n = 13	4.3 ± 0.3, n = 14
V:B below MLD	4.6* , n = 1	5.0 ± 0.2, n = 5
HB:AutoB	0.3 ± 0.01	0.1 ± 0.01
HNF	83.6 ± 3.7, n = 4 (83.6, 93.3)	150.7 ± 1.3, n = 6 (90, 237.3)
Ciliates	0.3 ± 0.01, n = 2 (0.3, 0.3)	0.5 ± 0.1, n = 3 (0.3, 0.6)
Dinoflagellates	0.1 ± 0.03, n = 2 (0.1, 0.2)	0.2 ± 0.1, n = 3 (0.1, 0.3)
ESD, Cil (µm)	25.1 ± 3.6, n = 202	20.9 ± 1.8, n = 299
ESD, Dino (µm)	26.4 ± 0.2, n = 71	27.8 ± 2.7, n = 108

4.3 Succession of heterotrophic biomass

4.3.1 Bacteria and viruses

Bacterial numbers at the initial measurements in end March/early April were low at all stations (2.0×10^5 to 3.4×10^5 cells ml^{-1}), corresponding well to those found in pre-bloom situation elsewhere in the North Atlantic (Seuhte et al., 2011; Bratbak et al., 2011). Later in April the concentration of bacteria increased significantly to about doble the amount in the upper mixed layer over 10 days at all stations (Icelandic Basin, t-test, $P < 0.0001$; Shetland Shelf, t-test, $P < 0.0001$; Norwegian Basin, t-test, $P = 0.0064$). Within the mixed layer, the highest concentrations of bacteria were found in the Norwegian Basin, and ranged from 3-6 x 10^5 cells ml^{-1}, whereas at the Shetland Shelf bacteria ranged from 3-5 x 10^5 cells ml^{-1}, and were lowest in the Icelandic basin, ranging from 2-4 x 10^5 cells ml^{-1} (fig.8). In contrast to the autotrophic plankton and the heterotrophic protists, bacteria were homogeneously distributed throughout the water coulmn (supp. 3), except in the Norwegian Basin, where a decrease in bacterial abundance was evident below 1000 m.

Viruses, considered to be mainly bacteriophages (Fuhrman 1999), largely followed the pattern of bacteria (supp. 2). The ratio of viruses to bacteria (V:B), however, decreased significantly during pre-bloom, and in the end of April reached values of 2.5-4.3 in the upper mixed layer. In the deep water V:B was generally higher, however, also decreased to 4.5-4.7 (table 2, 3, 4).

4.3.2 Heterotrophic protists

Heterotrophic protists were abundant throughout the mixed layer of the water column at all stations. Unidentified HNF were the most abundant group, followed by ciliates, and heterotrophic dinoflagellates. HNF were distributed evenly throughout the mixed layer, whereas μZP decreased exponentially towards the bottom of the mixed layer and with only few cells below (supp. 3). HNF were also abundant below the mixed layer, and even at depths below 1000 m, they were found in concentrations of 15-30 cells ml^{-1}.

Heterotrophic nanoflagellates

At the first visits to the deep basins, the abundance of HNF was relatively low throughout the mixed layer (22 and 40 cells ml^{-1} respectively). Within 2 to 3 weeks, however, the number increased 4 to 5 fold. At the first visit to the Shetland Shelf, the abundance

of HNF was higher (84 cells ml^{-1}) than at the two deep stations, and over the next 10 days, their abundance doubled, reaching the same concentration as at the two deep stations (fig.8). The size of HNF did not change during the period, but their body size tended to decrease slightly with depth: the mean diameter found at the surface was 3.2 μm ± 0.25, n = 99, while in samples deeper than 80 m it was 2.8 μm ± 0.01, n = 68. The mean diameter of all HNF (including all stations, depths and time) was 3.04 μm ± 0.31, n = 167.

Microzooplankton

For minimum of eight genera of ciliates and six genera of dinoflagellates were identified at the three sampling stations. In the Iceland Basin, small (<20 μm) ciliates, primarily *Strobilidium oviformis* and *Mesodinium* spp., and naked gymnodoid dinoflagellates dominated the μZP community in terms of abundance, while the main contributors to the μZP biomass were large (>20 μm) *Strombidium* spp. and *Mesodinium* spp. in the Norwegian Basin, ciliates of the genera *Strombidium, Mesodinium* and *Strobilidium* dominated the μZP community both in terms of biomass and numbers (see microscope images supp. 6).

In the Iceland Basin, the average ciliate abundance within the mixed layer ranged between 0.4 to 1.1 cells ml^{-1} with the maximum and minimum abundance occurring at the first visit and third visit at the station respectively. Despite the reduction in ciliate abundance, the overall biomass, estimated from ESD (table 2, 3, 4), increased during the period. The abundance of dinoflagellates (0.1-0.4 cells ml^{-1}) was always lower than the abundance of ciliates (fig.8).

In the Norwegian Basin, the average ciliate abundance within the mixed layer was twice as high as in the Iceland Basin, ranging between 2.1 and 3.0 cells ml^{-1} with maximum abundance occurring during the last visit (table 3). Similarly, dinoflagellates increased from 0.3 cells ml^{-1} at the first visit to 0.8 cells ml^{-1} at the last visit.

At the Shetland Shelf abundance of μZP was lower than at the deep basin stations ciliates ranging between 0.3-0.5 cells ml^{-1}, and dinoflagellates 0.1-0.2 cells ml^{-1}. While ciliates decreased, the dinoflagellates increased in abundance, concurrent with increase in diatoms.

Trophic status and state of the systems

Regarding the trophic status of the system, we found that the heterotrophic biomass (excluding mesozooplankton) exceeded the autotrophic biomass in the beginning of the period (table 2, 3, 4) similar to that found during "winter state" in Maixandeau et al., (2005) and in Iversen and Seuthe (2011). It is usually assumed that autotrophic production more or less balances community losses in the pre-bloom phase (Siegel et al., 2002). Autotrophs increased their dominance during pre-bloom and grew to comprise 50-80% of total biomass. Only the Norwegian Basin seemed to keep in balance with almost equal autotrophic and heterotrophic biomass throughout the period. We consider the three stations to reach in different stages of pre-bloom (illustrated as "succession line" fig.8), given the low Chl *a* (0.08 μg l^{-1}, high dominance of heterotrophs (biomass ratio of 2.9) in end-March at the Icelandic Basin, we denote it as winter state, following visits being in pre-bloom state. The Norwegian Basin remained in pre-bloom state at all visits, while we found the Shetland Shelf in a late pre-bloom state.

4.4 Microcosm experiments

Microcosm experiments 1, 2 and 3 were initiated on the 26.03, 11.04 and 21.04 respectively, and therefore the microbial community of the initial water varied in the three experiments (table 5). Temperature in the incubation tank was slightly higher during the first microcosm (10.4 °C ± 1.6) compared to the second (8.4 °C ± 1.1) and the third (8.1 °C ± 1). The initial concentration of nutrients was similar for all experiments; N=12, P=0.8, Si=4.3. Hereafter nutrients were depleted according to increasing biomass during the 10 d incubation periods. The nutrient values presented in the following are not corrected for the dilution of 10% vol. every second day. We observed clear differences between the treatments (hereafter called Treat<0.8, Treat<10, Treat<50) within the measured groups of microorganisms during the 10 d incubation. We also found Experiment 1 developed differently compared to the two later (fig. 9 and 10). Net growth rates were estimated only when periods of growth was evident (table 6). It should be noted that the separation of grazers by the screening method was not perfect, as small ciliates did pass the 10μm filter, why this treatment was not fully HNF-predator-free, explaining the decrease in HNF in Treat<10 after day 6 (fig. 10). The ciliate concentration, however, remained low in Treat<10; after 10 d reached <0.5 ciliates ml^{-1}, whereas the Treat<50 reached a concentration of 4.6 ciliates ml^{-1}.

Table 5: Initial cocentrations of Chl *a* (µg l^{-1}), autotrophs and heterotrophs (cells ml^{-1}) and V:B ratio of the three microcosm experiments shown as mean ± SD of the triplicates of each treatment (n = 3). * for Microcosm 2 only unfiltered samples were available for flow cytometer these were used as the initial values for pico sized organisms in Treat<10 and Treat<50, as the two other experiments show no significant difference between unfiltered and Treat<10 and Treat<50 in the initial abundance of pico sized organisms (P = 0.1178, 2way ANOVA). ** in Microcosm 3 there are no SD-values as only one sample of the triplicates at initiation of the experiment have been measured. NA = values not available.

	Microcosm 1			**Microcosm 2**			**Microcosm 3**		
Treatment:	**<0.8**	**<10**	**<50**	**<0.8**	**<10**	**<50**	**<0.8**	**<10**	**<50**
Total Chl *a*	0.002 ± 0	0.2 ± 0.002	0.3 ± 0.01	0.01 ± 0	0.7 ± 0.02	3.1 ± 0.1	0.02 ± 0	0.2 ± 0.3	0.5 ± 0.01
PicoE.	10 ± 0.1	3154 ± 205	2380 ± 326	NA	1859*	1859*	62**	2755**	2476
Synec.	101 ± 0.06	1147 ± 204	847 ± 37	NA	207*	207*	240**	2171**	2115
Nano phyto.	NA	571 ± 305	566 ± 129	NA	27*	27*	0**	350**	294
Bacteria	1.6 x 10^5± 0.1	1.4 x 10^5± 0.2	1.4 x 10^5± 0	2.7 x 10^5*	2.7 x10^5*	2.7 x10^5**	4.6 x 10^5**	3.9 x10^5**	3.4 x 10^5*
HNF	1.8	6.4	37.9	NA	40*	50.6**	NA	123**	167*
Ciliates	NA	NA	0.1	NA	NA	1 ± 0.3	NA	NA	1.1 ± 0.04
Dino.	NA	NA	0.1	NA	NA	1.2 ± 0.2	NA	NA	0.7 ± 0.2
V:B	15 ± 6	7 ± 0.6	8.6 ± 0.2	4.8*	4.8*	4.8**	3.6*	3**	2.6*

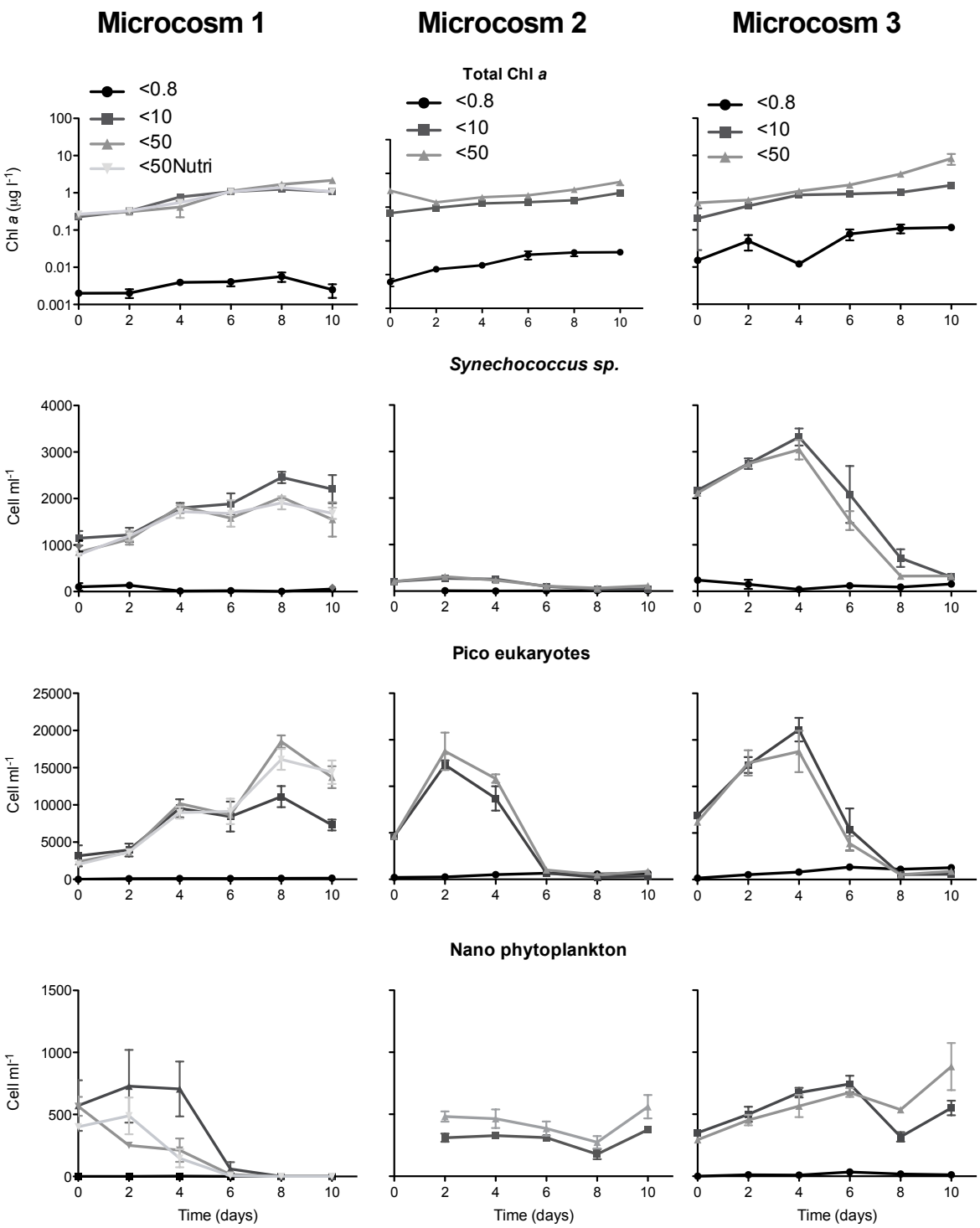

Figure 9: The development of autotrophs in the three microcosm experiments shown as the accumulated values, calculated according to Eq 2 and fig. 1. Total Chl *a* (log scale) and abundance of autotrophs represented as mean ± SE, n = 3 of triplicates of each treatment. Note different y-axis.

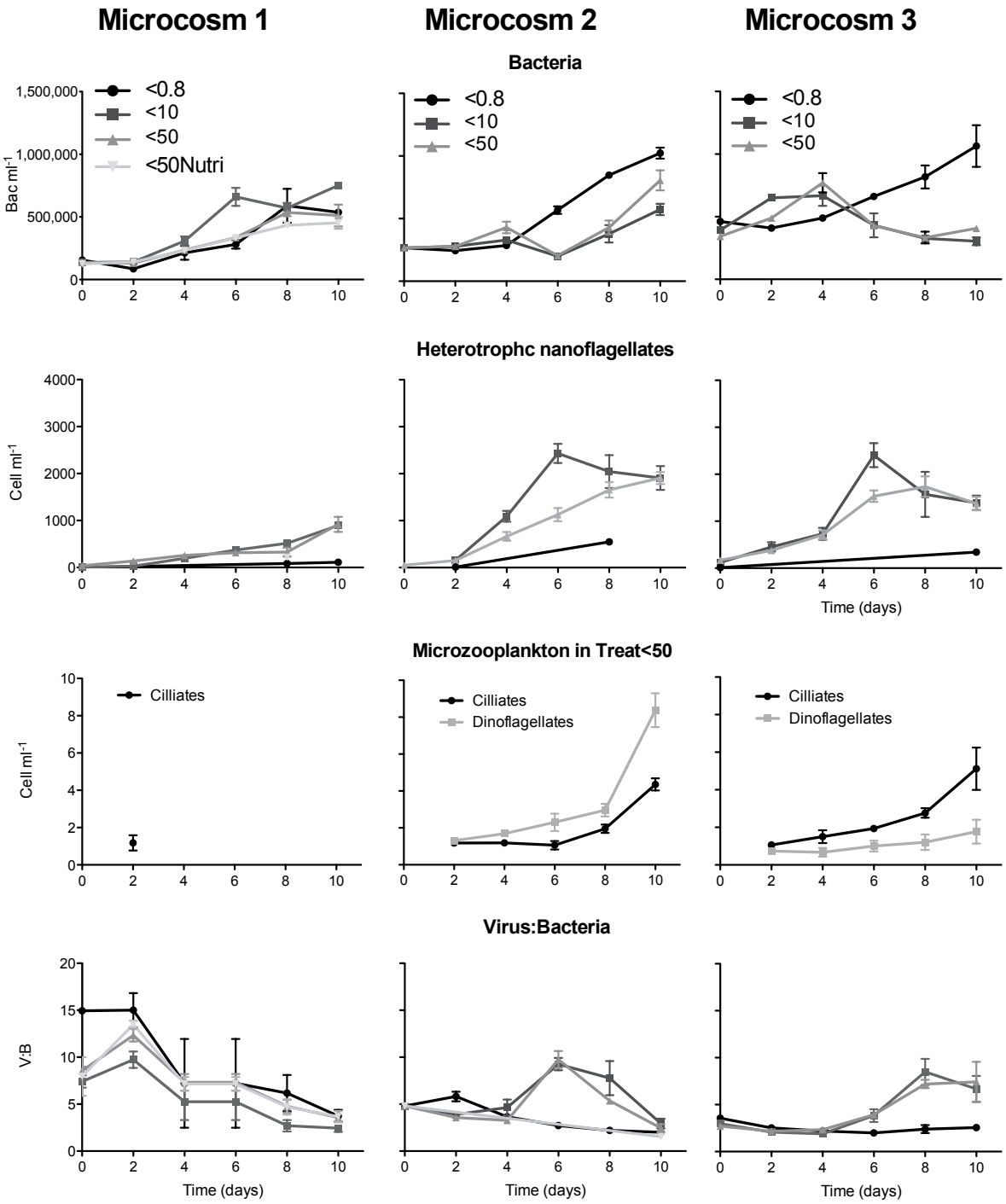

Figure 10: The development of heterotrophs in the three microcosm experiments shown as the accumulated values calculated according to Eq. 2 and fig.1. Heterotrophic protists and V:B are represented as mean ± SE, n = 3 of triplicates of each treatment. Microzooplankton are presented only from Treat<50. Note different y-axis.

Table 6: Net growth rates (d^{-1}) estimated from the three microcosm experiments by linear regressions to ln-transformed concentrations according to fig. 1. All fits were significant ($P < 0.005$). Growth rates represented as mean ± SD, n = 3 for all, except Microcosm 1 where Treat<50 and <50+Nutri. are joined, so n = 6. When growth rates were negative most of the incubation time, no numbers are given.

	Microcosm 1			**Microcosm 2**			**Microcosm 3**		
Treat:	<0.8	<10	<50	<0.8	<10	<50	<0.8	<10	<50
Chl *a*	0.13±0.03	0.18±0.02	0.24±0.06	0.15±0.03	0.11±0.01	0.16±0.02	0.49±0.5	0.29±0.27	0.34±0.2
PicoE.	0.26±0.06	0.18±0.04	0.25±0.02	0.16±0.03	-	-	0.24±0.03	-	-
Synec.	-	0.1±0.02	0.11±0.02	-	-	-	0.03±0.05	-	-
Bacteria	0.11±0.02	-	-	0.16±0.02	-	-	0.11±0.01	-	-
HNF	-	0.49±0.04	0.26±0.03	-	0.64±0.05	0.46±0.03	-	0.47±0.04	0.36±0.02
Ciliates	-	-	-	-	-	0.16±0.06	-	-	0.19±0.02
Dino.	-	-	-	-	-	0.21±0.04	-	-	0.11±0.05

Experiment 1

Relatively little biomass and little difference between screening-treatments were found in Experiment 1. Initial Chl *a* values were similar in Treat<10, Treat<50, Teat<50+nutrients (0.25 µg l^{-1} ± 0.02) (table 5), which after 10 days increased to an average of 1.4 µg l^{-1} ± 0.5 in all treatments, excluding Treat<0.8 (fig. 9). Nutrients did not decrease in any of the treatments; on the contrary, an increase was observed in Treat<0.8. There was no effect of nutrient addition (N = 20, P = 2, Si = 24.5) on the development of either autotrophic or heterotrophic biomass (fig. 9). The cumulative uptake, however, appears higher in treatments amended with nutrients (to be conclusive, the dilution needs to be taken into account, as it is responsible for a part of the nutrient decline). In contrast to the two later microcosm experiments, pico phytoplankton increased 4-7 fold in numbers until day 8, whereas HNF remained in relatively low abundance (< 500 cells ml^{-1} in the Treat<10, and <330 cell ml^{-1} in the Treat<50). Data of microzooplankton has not yet been processed for this experiment, but from first look it seemed that microzooplankton abundance decreased through the period, and both ciliates and dinoflagellates never exceeded 0.1 cells ml^{-1}.

Experiment 2

Initial concentration of Chl *a* were different after screening (table 5), and after 10 days Chl *a* increased to an average of 2.6 µg l^{-1} ± 0.3 in Treat<10, while Treat<50 reached 5.6 µg l^{-1} ± 1.6, with a high abundance of *Chaetoceros* spp. and *Pseudo-nitzschia* spp..

Nutrients decreased from initial conditions to N = 9.4 ± 0.6, P = 0.5 ± 0.03, Si = 3 ± 0.2 in Treat<50, and decreased slightly less in the Treat<10. Initial abundance of *Synechococcus* spp. was 5-10 fold lower than in the other two experiments, and remained low, while the pico eukaryotes peaked at day 2 and following decreased drastically. It was, however, possible to obtain net growth rates of the pico phytoplankton in Treat<0.8. There appeared to be a strong effect of the screening-treatment, as bacteria in Treat<0.8 (no grazers) exceeded bacteria in the larger screening 2-5 fold after 6 days. In Treat<10 and Treat<50, HNF increased exponentially until day 6 up to 2500 ± 300 cells ml^{-1} and decreased thereafter. μZP increased throughout the period and were dominated in numbers by dinoflagellates, which increased from 0.7 ± 0.2 to 8.4 ± 1.6 cells ml^{-1} after 10 days (fig.10).

Experiment 3

The sampled water used to set up the experiment contained less *Chaetoceros* spp. and more *Pseudo-nitzschia* spp., which was reflected in the initially less Chl *a* in Treat<50 than in experiment 2 (table 5). After 6 days, one of the Treat<50 replicates differed from the others and increased considerably in Chl *a* up to 13.5 μg l^{-1} (average of the three: 8.3 μg l^{-1} ± 3.8), and floating aggregates (of unidentified phytoplankton material, not Phaeocystis) could be observed in the bottles by the last sampling day. Treat<10 on the other hand only reached 1.6 μg l^{-1} ± 0.02 after 10 days. Nutrients in Treat<50 were depleted to N = 10.5 ± 0.4, P = 0.6 ± 0.03, Si = 3.4 ± 0.4, and not depleted at all in Treat<10. Pico phytoplankton development was similar to Experiment 2, only the period of growth lasted longer (4 days), after which they decreased to <1000 cells ml^{-1}. *Synechococcus* spp. were more abundant, but still 10 fold fewer than pico eukaryotes. Nanophytoplankton were more abundant (> 500 cells ml^{-1}) in this experiment than in the others, and especially high on the final sampling day (1260 cells ml^{-1}), in the same Treat<50 replicate that reached Chl *a* of 13.5 μg l^{-1}.

Heterotrophic protists increased in abundance as in experiment 2, only in this experiment ciliates dominated over dinoflagellates and had a higher net growth rate (0.2 d^{-1}), possibly causing stronger grazing on HNF, as these were generally less abundant in the Treat<10 and Treat<50 and had a lower net growth rates (table 6), yet reaching a similar max of 2380 ± 360 cells ml^{-1}. Bacteria increased similar to Experiment 2 in Treat<0.8, however, bacteria remained low in Treat<10 and Treat<50, whereas in Experiment 2, bacteria increased in these treatments after 6 days.

5 Discussion

While the North Atlantic spring bloom has been intensively studied, the pre-bloom dynamics, which set the scene for the spring bloom, has received far less attention. This study gives unique insight to pre-bloom conditions of the Subpolar North Atlantic Ocean, focusing on the microbial components as these dominate the system prior to the spring bloom. To our knowledge this is the first study of the area where all functional groups of the microbial food web have been enumerated. We document how the components of the microbial food web propagate in the window of pre-bloom from the end March to the beginning of May.

The following discussions focus on the succession of biomass at the three stations (fig. 11) and the trophic pathways the pre-bloom primary production undergoes by including the obtained experimental net growth and grazing rates (table 7).

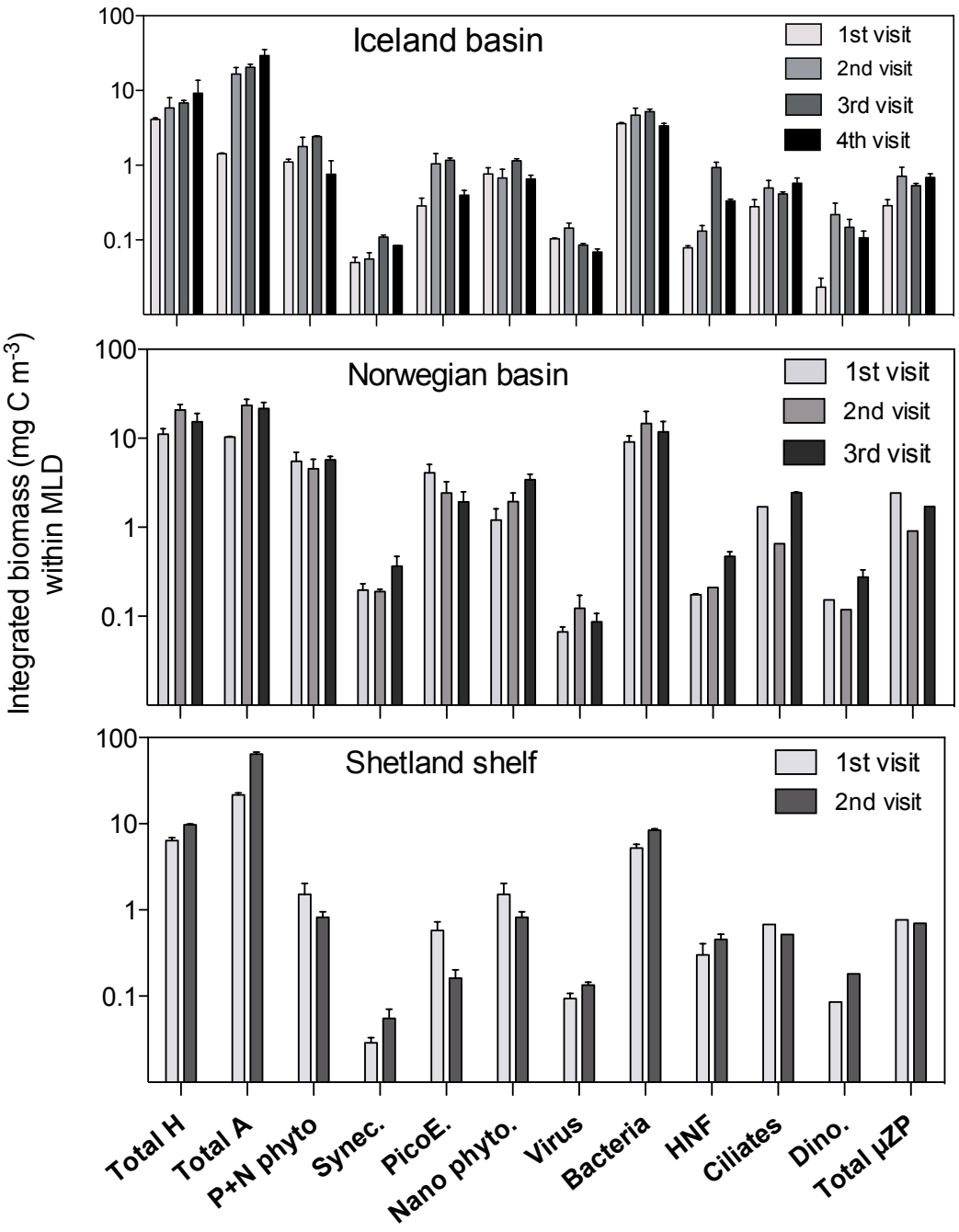

Figure 11: The development of integrated biomass at the three stations. Show it the sum of all sampled heterotrophs (H) and autotrophs (A) (- calulated from the total measured Chl *a*), the sum of pico and nano-phytoplankton (P+N phyto.), each of the three small phytoplankton and the heterotrophic protists. Values are calculated within the mixed layer of each station and shown in mg C m^3 as mean ± SD of the repeated profiles sampled during each visit.

5.1 Phytoplankton development

In the beginning of the survey all stations were in late-winter or pre-bloom conditions, with Chl *a* <0.5 μg l^{-1} and min. 85% of Chl *a* found in the less <10 μm fraction. Nutrients were evenly distributed and in high concentrations. As we proceeded into April, phytoplankton developed differently at the Iceland Basin, Norwegian Basin and on the Shetland Shelf, however consistent with previous studies within the same respective hydrographic regimes (Joint et al., 1993; Dale 1999; Sharples et al., 2006). A decrease in phototrophic pico eukaryotes towards the end of April was common for all stations, unlikely to be caused by light or nutrient limitation.

Norwegian Basin

Dale (1999) found that a bloom-maximum of 2.2 μg Chl *a* l^{-1} usually occurs in beginning of May in the Norwegian Basin (66°N, 2°E). Accordingly the system remained in pre-bloom state throughout our study with low Chl *a* (<0.55 μg l^{-1}), and the hydrography, nutrients, and total heterotrophic microbial biomass at this station did not change much over the sampling period (fig.8). The upper mixed layer was strongly dominated by pico eukaryotes, up to 20 x 10^3 cells ml^{-1}, equivalent to the maximum concentrations found in early May by the south coast of Norway (Bratbak et al., 2011) and Canadian Arctic waters in late summer (Trembley et al., 2009). When combining the biomass of pico- and nano phytoplankton (estimated from counts), these made up 70-30% of the total phytoplankton biomass (estimated from Chl *a*), and throughout the period a clear shift from a strong dominance of pico eukaryotic biomass to nano phytoplankton biomass was observed (fig. 8 and 9).

Icelandic Basin

We found max Chl *a* concentrations around 2 μg l^{-1} during April, even though there was strong influence of mixing and Chl *a* diluted out over min 600-350 m. Joint et al., (1993) found a max Chl *a* of 3 μg l^{-1} in early June in the Iceland Basin (60°N, 20°W) and Briggs et al., (2011) found the max bloom in mid May reaching a maximum of 5 μg l^{-1} in the same area (58.5–62.51°N, 18–28°W), thus we suspect the spring bloom may have taken off soon after our study terminated possibly concurrent with thermal stratification in agreement with Sverdrup (1953). In the end of March, the abundance of pico- and nano phytoplankton was low and Chl *a* <0.08 μg l^{-1}, even though the

abundance of grazers was low and nutrients were unlimited. Thus in this late winter period, phytoplankton growth was most likely limited by light. This is supported by the fact that the vertical mixing was deepest at this time (600 m). As the survey initiated only few days after equinox, potential light intensities were likely similar at all stations. Later in the period, pico- and nano phytoplankton were abundant throughout the mixed layer resulting in a relatively high integrated abundance (fig.11). As 8-14 days passed between visits it is possible that we missed a bloom of pico eukaryotes reaching similar concentrations to the ones observed in the Norwegian Basin.

Shetland Shelf

The Shetland Shelf is in general more productive than the deep basins and can reach Chl *a* levels of 12-15 μg l^{-1} during spring bloom, which usually occurs in mid-April (Sharples et al., 2006; Richardson et al., 2000; Radach and Piitsch 1997). This agrees with our observations, as we found the Shetland Shelf to have a faster response to the seasonal increase in sunlight, than the deep basin stations (fig.8). In mid-April we found high dominance of diatoms, Chl *a* up to 4.8 μg l^{-1} and a draw down of nutrients, our last visit most likely being right on the verge of spring bloom.

The main reason for the faster propagation is evidently that the shallow water column restrains mixing, in this case to 160 m. Another factor might be that be the shallowness of the Shelf, easily facilitates mixing to the bottom and thereby bringing up spores of larger phytoplankton and nutrients to the euphotic zone when assuming orbital motion of the mixing as argued in Backhaus (2003). The abundance of pico- and nano phytoplankton was low, which is to be expected in this "late-pre-bloom state" as pico- and nano phytoplankton prove to be most abundant under pre- and post bloom conditions (Joint et al., 1993; Gosselin et al., 1997) and contribute less in more productive systems (Agawin et al., 2000). As Shetland Shelf was only visited twice, and late-pre-bloom status already was reached by second visit, the two deep stations are more intensively investigated in regard to pre-bloom dynamics and effects of mixing.

5.1.1 Role of Deep Mixing

Sverdrup (1953) hypothesized that the initiation of the spring bloom occurs concurrently with the formation of a pycnocline, which, in the northern North Atlantic, is a thermocline. This theory holds in many cases and is often used i.e. in modeling. Our observations, however, show that production is likely to be important in a mixed water

column as well, and that autotrophic biomass here can exceed heterotrophic biomass well below the euphotic zone: first we found the Shetland Shelf station reached relatively high phytoplankton biomass within a 160 m fully mixed water column, with an integrated (to bottom) value of 10 g C m^{-2} ; second, the Norwegian Basin was the only station that was permanently stratified, and it had by far the lowest phytoplankton biomass, reaching a max integrated (100 m) value of 2 g C m^{-2} ; third, Iceland Basin had the deepest mixing - down to 600-300 m - throughout the period, nevertheless, the integrated phytoplankton biomass throughout the mixed layer was surprisingly high integrated (to MLD) values reaching 10 g C m^{-2} throughout April, thus the same as the shelf station in late pre-bloom conditions. It is beyond the scope of this study to compare autotrophic production to community respiration i.e. determining the critical depth and also to determine to what degree the deep mixed phytoplankton can add to the production or merely surviving (discussed further below).

Sverdrup's Critical Depth Hypothesis has been evaluated in several studies, e.g. Behrenfeld (2010), who argued that the highest primary production is more likely to occur in a deep mixed water column, where the grazers are diluted, than in a shallow stratified water-mass where increased grazing pressure leads to greater loss rates. Our results support that increased net phytoplankton growth is correlated with low biomass of heterotrophic protists within the mixed layer (fig. 11).

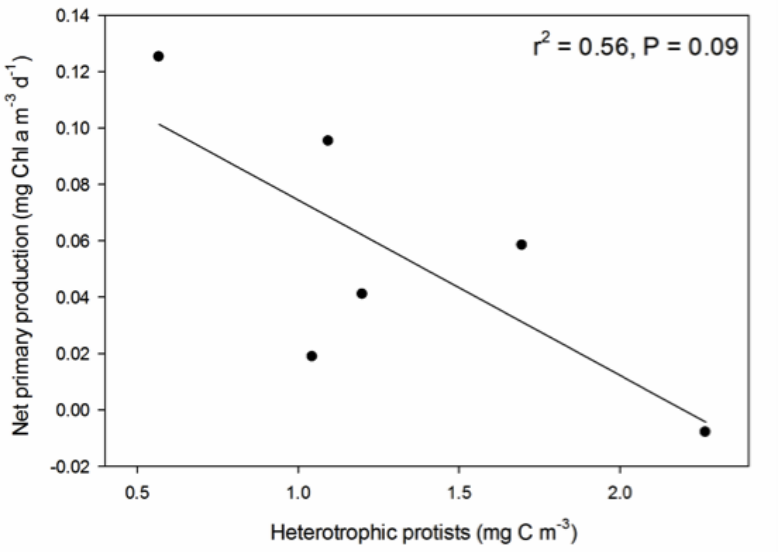

Figure 12: Net phytoplankton growth (mg Chl a $^{-3}$ d^{-1}) (on figure written as production) calculated as increase in Chl a between the different visits to the stations. Heterotrophic protist include ciliates, dinoflagellates and HNF.

In agreement with both Sverdrup (1953) and Behrenfeld (2010) it is possible that the stratification at the Norwegian Basin gives the pico phytoplankton a "head start" in the shallow upper mixed layer in the very early spring, explaining the relatively high Chl *a* already in March. However pico eukaryotes decrease gradually hereafter, most likely because of higher grazing pressure from the increasing number of HNF within the upper mixed layer.

During a survey in the same area of the Iceland Basin as our study, Backhaus et al. (1999) reported a spring production that began well before a seasonal thermocline had been established. During winter Backhaus et al., (2003) found living phytoplankton within the convective layer, down to 800 m, and links this to the orbital motions of the cells, which allows intermittent visits of plankton to the euphotic layer from much deeper depths. In this way the euphotic zone is "extended" and enables production over a great many meters of water column.

Dark periods may favor the small phytoplankton, as they have a relatively high affinity for light, and also do not have a cell wall, which obstruct light penetration (S. Rune Erga pers. comm.). As know for other phytoplankton as well, *Synechococcus* spp. and pico eukaryotes have been found to adapt to darkness by increasing their pigmentation (Campbell and Vaulot, 1993). Another trait helping to sustain life in a deeply mixed water column is that some small phytoplankton (<5 μm) can prey on bacteria, and to such degree that they are estimated to obtain 25 % of their biomass and even more of their nutrient demand via bacterivory (Zubkov and Tarran 2008). A North Atlantic (60°N) study showed that small phytoplankton became more bacterivory-dependent at depth when compared to the surface waters (Zubkov and Tarran 2008). The common pico eukaryote, *Micromonas pusilla*, has also been observed to ingest bacteria (Sherr and Sherr 2002).

5.2 Development of the heterotrophic communities

The heterotrophs varied in numbers within the upper mixed layer, while the abundances in the deep water did not change, indicating that the export production during pre-bloom was too low to give a response in abundance of heterotrophic protists in the deep, and not surprisingly, that changes in general are linked to primary production of the upper mixed layer. It is implied that all the following discussed changes occured within the upper mixed layer.

Ciliates and heterotrophic dinoflagellates

At all three stations, ciliates dominated the biomass of heterotrophic protists, except for a one-time dominance of HNF in the Icelandic Basin (fig. 11). The ciliate dominance was most pronounced in the Norwegian Basin, representing 65-85 % of the total heterotrophic biomass, whereas ciliate biomass only represented 30-75 % of the total heterotrophic biomass in the Icelandic Basin and 48-70 % on the Shetland Shelf. The generally high abundance of ciliates, especially in the Norwegian Basin, is consistent with the scientific consensus that, across the world oceans, ciliates dominate in less productive ecosystems characterized by high abundance of pico- and nanophytoplankton, whereas dinoflagellates dominate in eutrophic systems rich in diatoms (Calbet et al., 2008). The difference in the composition of the heterotrophic protists community can be explained by the difference between the feeding behaviors of ciliates and dinoflagellates: whereas ciliates prefer prey in the size range 2-10 μm, dinoflagellates are considered major grazers on diatoms, which are in their own size range (Hansen 1992), a strong correlation between ciliate abundance and their grazing on nano-plankton found in the Faroe-Shetland Channel by Kuipers et al., (2003), supports this assumption.

The succession of heterotrophic dinoflagellates mirrored the succession of the large-size phytoplankton, their abundance increasing towards the end of the investigated period. The shift in community composition was most pronounced in the Iceland Basin, where the integrated biomass of heterotrophic dinoflagellates increased 10 fold, a shift that could most likely be explained by the observed concurrent drastic increase in diatom abundance (from 1 to 200 cells ml^{-1}).

5.2.1 Controls of bacteria

At all times bacteria was the most prominent of the heterotrophic biomass, about double the biomass of all heterotrophic protists combined. Virus showed lowest biomass (0.1 mg C $m^{-3} \pm 0.04$, n = 27), though occasionally exceeding that of *Synechococcus* spp.

Our data suggests that bacteria in the winter state on the deep basins were C-limited, as the abundance of HNF was low (22-40 cells ml^{-1}) hence providing little top-down controle and as P was found in excess (0.8 μM). This would confirm that the increase of phytoplankton, from first to second visit, lead to a concurrent doubling of bacteria by supplying labile DOC. However a major difficulty linking DOC concentrations to availability or consumption rate, is that when bacteria are C-limited, an increase in DOC is probably an increase in the refractory part, and when new labile DOC is

supplied, it is readily used up, resulting in a more or less constant DOC concentration (supp. 7). Labile DOC supply in the surface layers is also supported by bacterial respiration (supp. 5), which appears to be 100 fold higher in the upper 100 m than in the aphotic zone of the Icelandic Basin.

By calculating bacterial carbon demand and assuming DOC to be the sole carbon source, we can conclude that new DOC must have been supplied in the pre-bloom e.g. in the Norwegian Basin between 1^{st} and 2^{nd} visit bacterial biomass increased from 9 to 15 mg C m^{-3}, assuming a growth efficiency of 15 % (del Giorgio and Cole 2000), this corresponds to a potential carbon uptake of 6 x 85 = 510 mg C m^{-3} over 10 days. In the same period DOC decreased from 512 to 507 mg C m^{-3}, indicating that the DOC supply over 10 days must have been in the same order of magnitude as the "standing stock" of DOC it self.

Same tendency was observed in experimentally, where water incubated from the "winter state" community in experiment 1 showed that bacterial abundance increased more in the Treat<10, than in the Treat<0.8 (no grazers) up to day 6, likely explained by the higher abundance of pico phytoplankton and therefore supply of DOC in Treat<10, whereas bacteria in Treat<0.8 incubated from this period were starving.

Virus-Bacteria ratio

It is generally thought that viruses are responsible for about 10-50 % of the total bacterial mortality in surface waters, and 50-100 % in environments where grazing protists are low in numbers e.g. the deep ocean (Fuhrman 1999). The higher the virus:bacteria (V:B) ratio, the higher bacteria mortality induced by strain specific viruses would be expected. Interestingly, during our study of the pre-bloom we found a decreasing V:B within the upper mixed layer at all stations, due to the increase in bacteria which was apparently not followed by an increase in viruses (while V:B below the mixed layer remained higher).

One explanation could be that the strains of bacteria that are the best competitors for the newly produced DOC become dominant over the strains that have been dominant during the winter, a strain specific virus may not yet have evolved for the new strains of dominating bacteria. The "lag-phase" of virus thus gives these bacteria a head start in pre-bloom phase. Eventually virus would most likely increase in numbers and according to 'Killing-the-Winner' hypothesis (Thingstad et al., 2000) become a regulation factor of the winning bacterial strains and the V:B would stabilize.

Bacterial biomass decreases in the upper mixed layer at the deep stations by the end of the period (fig.11). Since V:B is still low (i.e. virus is not considered a major regulating factor) and since DOC is most likely not limiting, it is likely to assume that the decrease of bacteria is caused by grazing from the increasing numbers of the heterotrophic nanoflagellates (to be discussed later). Hereby it can be argued that we see a shift in the control of bacteria; from bottom-up control (and possibly top down by virus) in the winter, to a top-down control by grazers within the pre-bloom phase.

5.3 Hetertrophic nanoflagellates

Among the heterotrophic protists, the largest increase (4-5 fold) both in abundance and biomass at all stations was observed for HNF. Estimates of HNF abundance vary widely depending on the system and season (Sanders et al., 1992). The concentrations found during our study are in the "low end" of those observed globally, but comparable to those found in other Northern marine systems (Vaqué et al., 2008; Seuthe et al., 2011). To our knowledge, this study is the first to provide data on HNF abundance in the Subpolar Atlantic during pre-bloom conditions. Concentrations up to 4-8 x 10^3 cells ml^{-1} have been measured in the Faroe-Shetland Channel in the summer (60-62 °N) (Kuipers et al., 2003), which suggests that the increasing trend in the concentration of HNF that we observed during pre-bloom might be sustained through the spring season, maintaining a high grazing pressure on bacteria and pico phytoplankton, and eventually reach similar concentrations to those found by Kuipers et al., (2003).

5.3.1 Prey-predator oscillations

The abundance of HNF did not show a strong linear correlation with Chl *a* concentration (P = 0.08), nor did it correlate with bacteria (P = 0.35) or pico eukaryote abundance (P = 0.7). The non-linear relationship between HNF and its prey may be explained by a natural oscillatory behavior in prey-predator systems ideally following a Lotka–Volterra relationship (Tanaka et al., 1997). Fenchel (1982) found a cyclical behavior between HNF and bacteria with a frequency of about 16 days. The biomass data (fig. 11) from the two deep stations tend to support such a cyclic relationship: within 22 days in the Norwegian Basin, the increase in bacteria lead to an increase in HNF, followed by a decrease in bacteria, and within 30 days in the Iceland Basin, the decrease in bacteria was followed by a decrease in HNF.

Another approach is to calculate the period of oscillation in a simple Lotka-Volterra

pair using the equation T = 2·π / √(growth rate of prey × mortality rate of predator), and the rates obtained via our microcosm experiments, were we estimated a net growth rate of 0.1 d^{-1} for bacteria, and assuming a mortality rate equal to the net growth rate for HNF of 0.5 d^{-1} (see table 3). Our calculations then yield an oscillation period of 25 days, which fits well with the observed oscillation.

The estimated bacterial net growth rate is possibly a "minimum" growth rate, as the bacteria in Treat<0.8 only had access to the existing DOC pool, whereas bacteria *in situ* could also take up DOC concurrently produced by phytoplankton and grazers. Furthermore, including the effects of heterotrophic ciliates and dinoflagellates in the system would increase the mortality of HNF, which together with a possibly higher *in situ* net growth rate of bacteria, would yield a period of oscillation shorter than our estimate of 25 days.

Andersen and Sørensen (1986) pointed out that the natural oscillatory behavior could be easily interrupted by the dynamic relation between HNF and their grazers, or by a rise in the carrying capacity of the prey, e.g. during spring bloom. An inverse relationship between HNF and ciliates was observed in the Iceland Basin during April (fig. 11), when a drop in the abundance of ciliates (most likely caused by the concurrent resurfacing of *Calanus finmarchicus*, which was observed, however is data not yet available) which may have opened a window for HNF to increase 10 fold to about 300 cells ml^{-1}, and after 10 days, the ciliates abundance increased again, leading to the abundance of HNF dropping to 100 cells ml^{-1}. The increase in HNF, however, does not appear to have a cascading effect on bacteria, suggesting that the two groups may not tightly be linked during pre-bloom conditions. As argued in Pernthaler (2005), the tight coupling between bacteria and HNF might only exist in low productive systems, in which HNF are bottom-up controlled by bacteria and not top-down controlled themselves.

5.4 Grazing estimates of HNF

HNF are usually perceived as being bacterivorous (implied grazing on heterotrophic bacteria), and thus most studies have focused on the HNF-bacteria trophic relationship (Fenchel 1982; Bjørnsen et al., 1988; Vaqué et al., 2008). HNF are, however, also known to be herbivorous, predating on pico eukaryotes (Sherr and Sherr 2002; Kuipers et al., 2003; Brek-Laitinen and Ojala 2011) and phototrophic bacteria, e.g. *Synechococcus* spp. (Caron et al., 1991; Christaki et al., 2001; Worden and Binder, 2003). It is challenging

to distinguish between HNF predation on bacteria and phytoplankton, although it has been attempted (Caron et al., 1991; Christaki et al., 2001). The average diameter of HNF in our study (3.04 μm ± 0.31, n = 167) agrees with the ≤ 3μm average size obtained by Jürgens and Massana (2008) for 76% of HNF across four different marine areas. The authors speculated that the estimated HNF average size may be too small for HNF to be able to ingest pico phytoplankton, yet HNF with a diameter of 2-5 μm have been observed to ingest 1.5-2 μm diameter pico eukaryotes and coccoid cyanobacteria (Sherr et al., 1997). Thus we believe that size did not hinder HNF herbivory in the system we studied, which is supported by the results of our grazing experiments. Our estimates of HNF grazing (table 7) were based on the differences between the number of bacteria and pico-phytoplankton in the 0.8 μm (predator free) and in the <10 μm (HNF present) pre-screened seawater, calculated by Eq. 3 and 4. Same "screening-method" was used by Christaki et al. (2001), who evaluated it to give similar results to those obtained by measuring consumption of fluorescently labeled bacteria (FLB). The data obtained from the microcosm experiments provide evidence that HNF grazed heavily not only on heterotrophic bacteria, but also on *Synechococcus* spp. and pico eukaryotes.

Table 7: Clearance and ingestion rates of HNF on prey-specific items, calculated from the three microcosm experiments (mean ± SE, n = 3) according to Eq. 3 and Eq. 4 respectively. Specific clearance is given as body vol^{-1} h^{-1} HNF^{-1} and also shown as volume (nl). Community clearance is the % standing stock of prey consumed d^{-1}. % carbon uptake via the three prey categories are calculated from ingestion rates and specific carbon content of the prey. The last row shows ciliate grazing on HNF from Experiment 3.

Prey	**Ingestion rate (prey HNF^{-1} h^{-1})**	**Clearance rate (x body vol h^{-1})**	**Clearance rate (nl HNF^{-1} h^{-1})**	**Community clearace d^{-1}**	**% HNF carbon uptake**
Microcosm 1					
Bacteria	1.9 ± 162	2.7 x 10^5	5	2 ± 12	-
Microcosm 2					
Bacteria	1 ± 23	2 x 10^5	4	10 ± 15	43
Pico eukaryotes	0.06 ± 0.9	1.1 x 10^6	22	57 ± 27	54
Synechoccus spp.	0.02 ± 0.3	2.6 x 10^6	52	41 ± 78	3
Microcosm 3					
Bacteria	4 ± 25	3.6 x 10^5	7	21 ± 3	68
Pico eukaryotes	0.07 ± 1.8	1.3 x 10^6	25	45 ± 23	29
Synechoccus spp.	0.03 ± 0.8	9 x 10^5	18	33 ± 29	3
Ciliates -> HNF	1.8 ± 30	8 x 10^4	3524	13 ± 8	-

HNF grazing rates: Bacteria

Our estimates of HNF ingestion rate (1-4 bacteria h^{-1}) is in the range of that found in other studies (Bjørnsen et al., 1988; Christaki et al., 2001; Vaqué et al., 2008). HNF grazing on bacteria increased 10 fold through the study period, from 2% d^{-1} of the bacteria standing stock in the fist experiment, to grazing 21% d^{-1} in the last experiment. This increase in the capacity of HNF grazing on bacteria may be best explained by the observed concurrent exponential increase in HNF abundance.

HNF grazing rates: pico phytoplankton

HNF grazed 33-40 % of the pico-phytoplankton standing stock d^{-1}, which is within the range although slightly higher than the 0.5-45% (mean 13 %) clearance rate obtained by Christaki et al. (2001) and the 33% ± 11 d^{-1} rate obtained by Worden and Binder (2003) for *Synechococcus* spp. For pico eukaryotes, we could not find any clearance rates in the literature to compare our estimates to. The HNF ingestion rate of bacteria was 2-5 magnitudes greater than that of pico phytoplankton, and the ingestion rate of pico eukaryotes was twice as high as of *Synechococcus* spp., reflecting a difference in abundance, i.e. encounter rate, rather than HNF prey selectivity.

5.5 HNF's carbon sources

The carbon demand of HNF can be calculated assuming an average doubling time for HNF of 1.3 days (calculated from microcosm experiments treatment 10), a gross growth efficiency of 30% (Fenchel 1982), a mean volume of 20 μm^3 ± 4 (our own measurement) a conversion factor to carbon biomass of 220 fg C μm^{-3} (Børsheim and Bratbak 1987) (resulting in 3.24 pg C HNFμm^{-1}), and a carbon content of 20 fg $cell^{-1}$ for bacteria (Lee & Fuhrman 1987), the daily carbon demand of HNF can be estimated to be 4237 fg C d^{-1}, equaling 9 bacteria h^{-1}. Given the estimated ingestion rate of bacteria (max. 4 bacteria h^{-1}), consumption of bacteria is evidently not enough to satisfy HNF carbon demand at their estimated net growth rate. To make up for the missing carbon would require HNF to ingest 0.2 pico phytoplankton h^{-1}, a rate that is within the same order of magnitude as the HNF ingestion rate we found for pico phytoplankton, thus confirming that the carbon demand of HNF was satisfied by both bacteria and pico phytoplankton.

We found an almost equal part of HNF carbon uptake derived from pico eukaryotes (42%) and bacteria (55%), a larger estimate than the 27% pico-phytoplankton carbon

uptake estimate Christaki et al. (2001) obtained in a system dominated by photosynthetic prokaryotes, suggesting that pico eukaryotes may be a better food item than photosynthetic prokaryotes i.e *Synechococcus* spp.. Despite the similarity between our estimates and published rates, we found that only 3% of HNF carbon uptake was via *Synechococcus* spp., presumably caused by the fact that *Synechococcus* spp. in our system proved to have low net growth rate and low abundance, as well as low carbon content cell^{-1}, 4 times lower than pico eukaryotes. In addition, in culture studies, *Synechococcus* has been described as a poor food item for protists grazers (Caron et al., 1991), yet we could not detect any HNF as community showed selection against *Synechococcus* spp.

A rough estimate shows that in our experiments, about 5 times more carbon was available in the form of bacteria than bound in pico eukaryotes, the discrepancy between available carbon and the measured uptake suggest that HNF were actively selecting for pico eukaryotes. It should, however, be considered that the net growth rate of pico eukaryotes (0.2 d^{-1} $\pm$ 0.03) was double that of bacteria (0.1 d^{-1} $\pm$ 0.02), thus accelerating uptake of pico eukaryotes.

Theoretical vs. experimental measures of grazing

Our grazing estimates of HNF grazing on bacteria and pico phytoplankton agree with the range given in Kiørboe (2011), which as well are calculated according to Hansen et al. (1997). The volume-specific clearance rates for HNF are 2-10 times higher that the "theoretical" value of 10^5 x body volume h^{-1} (Fenchel 1982). Fenchel's value, however, was obtained in an experiment with concentrations of bacteria and HNF 10 fold higher than our experiments, therefore the obtained cleared volume may naturally have been smaller, than in our more dilute experiment. At high food concentration, the clearance rate may become less than maximal due to saturation of the digestion system or prey-handling processes (Kiørboe 2011).

Applying a theoretical value may give an idea of the potential grazing of HNF, but the factual value is very likely different, depending on the state of the environment, as well as the taxonomical composition of HNF and its prey. Based on our in situ measurements of integrated biomass, it is evident that pico eukaryotes were abundant during the pre-bloom, comprising up to about half of the total biomass available for HNF, therefore also likely to comprise a important part of HNF's diet. The coupling between HNF and pico eukaryotes seemed to be stronger than their coupling with

bacteria. Based on the difference in numbers of HNF between treatments with and without predator (ciliate), were found ciliates to clear 13% of HNF standing stock h^{-1}. If the rates we obtained were to be applied in a system analysis, top-down control on HNF by ciliates should as well be considered.

5.6 Concluding remarks

We found that the pre-bloom period of the Subpolar North Atlantic was productive and highly dynamic, therefore challenging the view that "diatom blooms in spring are the beginning of the seasonal cycle" (Edward and Richardson, 2004). Additionally we found that pico-sized phytoplankton dominated the pre-bloom phytoplankton biomass and, given their high turnover rates, most likely an even larger part of the primary production.

Grazing estimates revealed that pico phytoplankton was rapidly grazed by heterotrophic nanoflagellates, removing up to 50% of standing stock d^{-1}, and grazing of ciliates on heterotrophic nanoflagellates was also evident. This is likely the reason why the phytoplankton production does not lead into a bloom situation with high phytoplankton biomass.

Thus in the pre-bloom period, production enters the ocean food web via nano-sized microorganisms and therefore, in comparison to the diatom spring blooms, remain more "invisible". Nevertheless the pre-bloom production feeds a growing quantity of heterotrophic protists. These have a strong link to mesozooplankton (Levinsen and Nielsen 2002; Calbet 2008) and there is evidence that copepods feed preferentially on the nitrogen-rich protists rather than phytoplankton, when the two are found in similar quantities (Atkinson 1994; Gifford and Dagg 1991), therefore the link between the production of the pre-bloom and higher trophic levels is possibly strong.

In regard to the increasing evidence and consideration of climatic change impact on the timing and trophic mismatch of marine plankton (Edward and Richardson, 2004), e.g. the potential asynchrony between the timing of spring bloom and the resurfacing the diapausing *Calanus finmarchicus,* it should be considered to which degree the pico phytoplankton are able to fuel the part of a food web that may benefit the mesozooplankton and thus prevent severe consequences of a mismatch.

6 References

Andersen, P. and Sørensen, H.M. 1986. Population dynamics and trophic coupling in pelagic microorganisms in eutrophic coastal systems. Mar Ecol Prog Ser. 33:99-109

Agawin, N.S.R., Duarte, C.M., Agusti, S. 2000. Nutrient and temperature control of the contribution of picoplankton and phytoplankton biomass and production. Limnol Oceanogr. 45:591-600

Akinson, A. 1996. Subantarctic copepods in an oceanic, low chlorophyll environment: ciliate predation, food selectivity and impact on prey populations. Mar Ecol Prog Ser. 130: 85-96

Azam, F., Fenchel, T., Field, J.G., Gray, J. S., Meyer-Reil, L. A., Thingstad, F. 1983. The Ecological Role of Water-Column Microbes in the Sea. Mar Ecol Prog Ser. 10:257-263

Backhaus, J. Hegseth, E.N., Wehde, H., Irigoien, X., Hatten, K., Logemann, K. 2003. Convection and primary production in winter. Mar Ecol Prog Ser. 251:1-14

Behrenfeld, M. J. 2010. Abandoning Sverdrup's Critical Depth Hypothesis on phytoplankton blooms. Ecology. 91:977–989

Bendtsen, J., Lundsgaard, C., Middelboe, M., Archer, D. 2002. Influence of bacterial uptake on deep-ocean dissolved organic carbon. Global Biogeochem. Cycles. 16(4):1-8

Blanchot, J., Andre, J.M., Navarette, C., Neveux, J., and Radenac, M.H. 2001. Picophytoplankton in the equatorial Pacific: vertical distributions in the warm pool and in the high nutrient low chlorophyll conditions. Deep-Sea Res. I 48:297-314

Blindheim, J. and Østerhus, S. 2005. IN: The Nordic seas: an integrated perspective: oceanography, climatology. Helge Drange.

Billett, D.S.M., Lampitt, R.S., Rice, A.L., Mantoura, R.F.C. 1984. Seasonal sedimentation of phytoplankton to deep-sea benthos. Nature. 302:520-522

Bjørnsen, P.K., Riemann, B. Horsted, S.J., Nielsen, T.G., Pock-Sten, J. 1988. Trophical interactions between heterotrophic nanoflagellates and bacterioplankton in manipulated seawater enclosures. Limnol Oceanogr. 33:409-420

Braarud, T., Nygaard, I. 1978. Phytoplankton observations in offshore Norwegian costal waters between 62°N and 69°N. Fisk-dir. Havunders. 16:489-505

Bratbak, G., Heldal, M., Thingstad, T. F., Riemann, B. Haslund, O.H. 1996, Dynamics of virus abundance in coastal seawater. FEMS Microbiol Ecol. 19:263-269

Bratbak G., Jacquet S., Larsen A., Pettersson L.H., Sazhin A.F., Thyrhaug R., 2011. The plankton community in Norwegian waters – abundance, composition, spartial distribution and dial variation. Cont. Shelf Res 31:1500-1514

Brek-Laitinen, G. and Ojala, A. 2011. Grazing of heterotrophic nanoflagellates on the eukaryotic picoautotroph Choricystis sp. Aquat Microb Ecol. 62:49-59

Briggs, N., Perry, M.J., Cetinic, I., Lee, C., D'Asaro, E., Gray, A.M, Rehm, R. 2011. High-resolution observations of aggregate flux during a sub-polar North Atlantic spring bloom. Deep-Sea Res. I 58:1031-1039

Brussaard, C.P.D., 2004. Optimization of Procedures for Counting Viruses by Flow Cytometry. Appl Environ Microbiol. 70:1506-1513

Børsheim, K.Y. and Bratbak, G. 1987. Cell volume to cell carbon conversion factors for a bacterivorous Monas sp. enriched from seawater. Mar Ecol Prog Ser. 36:171-175

Calbet, A. 2008. The trophic roles of microzooplankton in marine systems. ICES Journal of Marine Science. 65: 325–331.

Campbell, L. and Vaulot, D. 1993. Photosynthetic picoplankton community structure in the subtropical north Pacific Ocean near Hawaii (station ALOHA). Deep-Sea Res. 40:2043-2060

Caron, D.A., Lim, E.L., Miceli, G., Waterbury, J.B., Valois. F.W. 1991. Grazing and utilization of chroococcoid cyanobacteria and heterotrophic bacteria by protozoa in laboratory cultures and a coastal plankton community. Mar. Ecol. Prog. Ser. 76:202-217

Christaki, U., Giannakourou, A., van Wambeke, F. Grégori, G. 2001. Nanoflagellate predation on auto- and heterotrophic picoplankton in the oligotrophic Mediterranean Sea. J Plankton Res. 23(11):1297-1310

Cottrell, M.T., Michelou, V.K., Nemcek, N., DiTullio, G., Kirchman, D.L. 2008. Carbon cycling by microbes influenced by light in the Northeast Atlantic Ocean. Aquat Microb Ecol. 50:239-250

Dale T., Rey F., Heimdal, B.R. 1999. Seasonal development of phytoplankton at a high latitude oceanic site. Sarsia. 84:419-435

de Boyer Montégut, C., Madec, G. Fischer, A. S., Lazar, A., Iudicone, D. 2004. Mixed layer depth over the global ocean: An examination of profile data and a profile-based climatology, J. Geophys. Res., 109, C12003, doi:10.1029/2004JC002378

del Giorgio, P., and J.J. Cole. 2000. Bacterial energetics and growth efficiency. In D. L. Kirchman (ed.), Microbial Ecology of the Oceans, 1st edn. Wiley-Liss, pp. 289-325.

Ducklow, H. W. 1983. The production and fate of bacteria in the ocean. Bioscience. 33:494-501

Edwards, M. and Richardson, A.J. 2004. Impact of climate change on marine pelagic phenology and trophic mismatch. Nature. 433: 881-883

Fenchel, T. 1982. Ecology of Heterotrophic Microflagellates. IV. Quantitative Occurrence and Importance as Bacterial Consumers. Mar Ecol Prog Ser. 9:35-42

Frost, B.W. 1972. Effects of size and concentration of food particles on the feeding behavior of the marine planktonic copepod calanus pacificus. Limnol Oceanogr. 17(6):805-815

Fuhrman, J.A. 1999. Marine viruses and their biogeochemical and ecological effects. Nature. 399:541-548

Gifford, D.J., Dagg, M.J. 1991. The microzooplankton-mesozooplankton link: consumption of planktonic protozoa by the calanoid copepods Acartia tonsa Dana and Neocalanus plumchrus Murukawa. Mar Microb Food Webs. 5: 161-177

Gosselin, M., Levasseur, M., Wheeler, P.A., Horner, R.A., Booth, B.C. 1997. New measurements of phytoplankton and ice algal production in the Arctic Ocean, Deep-sea Res. II 44:1623-1644

Radach, G. and Piitsch, J. 1997. Climatological annual cycles of nutrients and chlorophyll in the North Sea. J Sea Res. 38:231-248

Hansen, B., and Østerhus, S. 2000. North Atlantic – Nordic Seas exchanges. Prog Oceanogr. 45:109-208

Hansen, P.J. 1992. Prey size selection, feeding rates and growth dynamics of heterotrophic dinoflagellates with special emphasis on Gyrodinium spirale. Marine Biology. 114:327-334

Hansen, P.J., Bjønsen, P.K., Hansen, B.W. (1997). Zooplankton grazing and growth: Scaling within the 2–2,000 μm body size range. Limnol Oceanogr. 42:687-704

Hansell, D.A., Carlson, C.A., Repeta, D.J., Schlitzer, R. Dissolved organic matter in the ocean- a controversy stimulates new insights. Oceanography 22(4):202-211

Iriarte, A., Sarobe, A., Orive, E. 2008. Seasonal variability in bacterial abundance, production and protistan bacterivory in the lower Urdaibai estuary, Bay of Biscay. Aquat Microb Ecol. 52: 273-282

Iversen, R.K. and Seuthe, L. 2011. Seasonal microbial processes in a high-latitude fjord (Kongsfjorden, Svalbard): I. Heterotrophic bacteria, picoplankton and nanoflagellates. Polar Biol. 34:731–749

Jacquet, S., Havskum, H., Thingstad, T. F., Vaulot, D. 2002. Effects of inorganic and organic nutrient addition on a coastal microbial community (Isefjord, Denmark). Mar Ecol Prog Ser. 228:3-14

Jespersen A.M. and Christoffersen K., 1987. Measurements of chlorophyll-a from phytoplankton usin ethanoal as extraction solvent. Arch. Hydrobiol. 109(3):445-454

Joint, I., Pomroy, A. Savidge, G. Boyd, P. 1993. Size-fractionated primary productivity in the northeast Atlantic in May-July 1989. Deep-Sea Res. II 40:423-44

Jürgens, K. and Massana, R. 2008. Protist grazing on marine bacterioplankton. In: D. L. Kirchman (ed.) Microbial Ecology of the Oceans. 2nd edn. Wiley-Liss.

Kiørboe, T., Møhlenberg, F., Nicolajsen, H. 1982. Ingestion rate and gut clearance in the planktonic copepod Centropages hamatus (Lilljeborg) in relation to food concentration and temperature. Ophelia. 21:181–194

Kiørboe, T. 2011. How zooplankton feed: mechanisms, traits and trade-offs. Biol. Rev. 86: 311–339

Koroleff, F., 1983. Determination of silicon. IN Methods of seawater Analisys. 2. ed., Verlag Chemie

Kuipers, B., Witte, H., Noort, v.G, Gonzalez, S. 2003. Grazing loss-rates in pico- and nanoplankton in the Faroe-Shetland Channel and their different relations with prey density J. Sea Res. 50(1):1-9.

Lee, S., Fuhrman J.A., 1987. Relationships between biovolume and biomass of naturally derived marine bacterioplankton. Appl Environ Microbiol 53:1298-1303

Levinsen, H. and Nielsen, T.G. 2002. The trophic role of marine pelagic ciliates and heterotrophic dinoflagellates in arctic and temperate coastal ecosystems: a cross-latitude comparison. Limnol. Oceanogr. 47:427-439

Li, W.K.W, McLaughlin, F.A, Lovejoy, C., Carmack, E.C. 2009. Smallest Algae Thrive as the Arctic Ocean Freshens. Science. 326:539

Longhurst, A. 1995. Seasonal cycles of pelagic production and consumption. Prog Oceanogr. 36:77-167

Maixandeau, A., Lefèvre, D., Hera Karayanni, H., Christaki, U., Wambeke, V.W., Thyssen, Denis, M., Fernández, C.I., Uitz, J., Leblanc, K., Quéguiner, B. 2005. Microbial community production, respiration, and structure of the microbial food web of an ecosystem in the northeastern Atlantic Ocean. J Geoph. Res. 110: C07s17

Menden-Deuer, S. and Lessard, E.J. 2000. Carbon to volume relationships for dinoflagellates, diatoms, and other protist plankton. Limnol. Oceanogr. 45(3):569-579

Murphy, J. and Riley, J.P. 1962. A modified single solution method for the determination of phosphate in natural waters. Anal. Chim. Acta 27:31-36

Nagata, T. 2000. Microbiology of the oceans, edited by Kirchman, D. L., Wiley-Liss, Inc., New York

Richardson, K., Visser, A.W., Pedersen, F.B. 2000. Subsurface phytoplankton blooms fuel pelagic production in the North Sea. J Plankton Res 22(9):1663-1671

Robertson J.E., Watson A.J., Langdon, C., Ling, R.D., Wood, J.W. 1993. Diurnal variation in surface pCO2 and 0 2 at 60°N, 20°W in the North Atlantic. Deep-Sea Res. II 40:409-422

Pernthaler, J. 2005. Predation on prokaryotes in the water column and its ecological implications. Nature Reviews Microbiology. 3(7):537-546

Pomeroy, L.R.1974. The ocean'sfood web, a changing paradigm. BioScience. 24(9):499-504

Porter, K.G. and Feig, Y.S., 1980. The use of DAPI for identifying and counting aquatic microflora. Limnol. Oceanogr. 25:943-948

Putt, M. and Stoecker, D.K. (1989) An experimentally determined carbon:volume ratio for marine 'oligotrichous' ciliates from estuarine and coastal waters. Limnol. Oceanogr. 34:1097-1103

Sanders, R.W., Caron, D.A., Berninger, U.G. 1992. Relationships between bacteria and heterotrophic nanoplankton in marine and fresh waters: an inter-ecosystem comparison. Mar. Ecol. Prog. Ser. 86:1-14

Seuthe, L., Töpper, B., Reigstad, M., Thyrhaug, R., Vaquer-Sunyer, R. 2011. Microbial communities and processes in ice-covered Arctic waters of the northwestern Fram Strait (75 to 80° N) during the vernal pre-bloom phase. Aquat. Microb. Ecol. 64:253-266

Shaples, J., Ross, O.N., Scott, B.E., Greenstreet, S. P. R., Fraser, H. 2006. Inter-annual variability in the timing of stratification and the spring bloom in the North-western North Sea. Cont. Shelf Res. 26:733-751

Sherr, E.B., Sherr, B.F., Fessenden, L. 1997. Heterotrophic protists in the central Arctic Ocean. Deep-Sea Res. II 44:1665-1682

Sherr, E.B. and Sherr, B.F. 2002. Significance of predation by protists in aquatic microbial food webs. Antonie Leeuwenhoek. 81:293-308

Sieburth, J. McN., Smetacek, V., Lenz, J. 1978. Pelagic Ecosystem Structure: Heterotrophic Compartments of the Plankton and Their Relationship to Plankton Size Fractions. Limnol. Oceanogr. 23:1256-1263

Siegel, D.A., Doney, S.C., Yoder, A., 2002. The North Atlantic Spring Phytoplankton Bloom and Sverdrups Critical Depth. Science. 296:730-733

Sorokin, Y.I. 1977. The heterotrophic phase of plankton succession in the japan sea. Marine Biology 41:107-11

Stefánsson, U. 1968. Dissolved nutrients, oxygen and water masses in the Northern Irminger Sea. Deep Sea Res Oceanogr Abstr. 15:541-575

Steele, J.H., 1974. The structure of marine ecosystems. Cambridge, Harvard University Press.

Stoecker, D.K., Gifford, D.J., Putt, M. 1994. Preservation of marine planktonic ciliates: losses and cell shrinkage during fixation. Mar Ecol Prog Ser. 110:293-299

Sverdrup, H.U. 1953. On conditions for the vernal blooming of phytoplankton. Journal du Conseil International pour l'Exploration de la Mer. 18:287-295

Tanaka, T., Fujita, N., Taniguchi, A. 1997. Predator-prey eddy in heterotrophic nanoflagellate- bacteria relationships in a coastal marine environment: a new scheme for predator-prey associations. Aquat Microb Ecol 13:249-256

Tarran, G.A., Zubkov, M.V., Sleigh, M.A., Burkhill, P.H., Yallop, M. 2001. Microbial community structure and standing stocks in the NE Atlantic in June and July of 1996. Deep-Sea Res. II 48:963-985

Tarran, G.A., Heywood, J.L., Zubkov, M.V. 2006. Latitudinal changes in the standing stocks of nano- and picoeukaryotic phytoplankton in the Atlantic Ocean. Deep-Sea Res. II 53:1516-1529

Thingstad, T.F. 2000. Elements of a theory for the mechanisms controlling abundance, diversity, and biogeochemical role of lytic bacterial viruses in aquatic systems. Limnol Oceanogr. 45:1320-1328

Tremblay, G., Belzile, C. Gosselin, M., Poulin, M., Roy, S., Tremblay, J.E. 2009. Late summer phytoplankton distribution along a 3500 km transect in Canadian Arctic waters: strong numerical dominance by picoeukaryotes. Aquat Microb Ecol. 54: 55–70

Vaqué, D., Guadayol, Ò., Peters, F., Felipe, J., Angel-Ripoll, L., Terrado, R., Lovejoy, C., Pedrós-Alió, C. 2008. Seasonal changes in planktonic bacterivory rates under the ice-covered coastal Arctic Ocean. Limnol Oceanogr. 53:2427-2438

Verity, P.G. and Langdon, C. 1984. Relationships between lorica volume, carbon, nitrogen, and ATP content of tintinnids in Narragansett Bay. J Plankton Res. 6:859-868.

Wood, E.D., Armstrong, F.A.J., Richards, F.A. 1967. Determination of nitrate in sea water by cadmium- copper reduction to nitrite: Journal of Marine Biological Association, U.K.

Worden, A.Z. and Binder, B.J. 2003. Application of dilution experiments for measuring growth and mortality rates among Prochlorococcus and Synechococcus populations in oligotrophic environments. Aquat Microb Ecol. 30: 159–174

Zubkov, M.V., Burkill, P.H., Topping, J.N., 2006. Flow cytometric enumeration of DNA-stained oceanic planktonic protists. J Plankton Res 29:79-86

Zubkov, M.V., Tarran, G.A. 2008. High bacterivory by the smallest phytoplankton in the North Atlantic Ocean. Nature. 455:224-226

7 Supplementary

Supplementary 1

Nutrients and dissolved organic carbon at the three stations during the studied period. Concentrations are shown both within and below the mixed layer depth as averagde (mean ± SD, n) concentration of nitrate+nitrite, phosphate, silicate, DOC (dissolved organic carbon) and TDN (total dissolved nitrogen) all in μM.

Iceland Basin	**1st visit**	**2nd visit**	**3rd visit**	**4th visit**
MLD	618 m	493 m	492 m	344 m
NO_3^-	12.57 ± 0.2, n = 12	12.37 ± 0.52, n = 23	12.13 ± 0.51, n = 22	11.86 ± 0.57, n = 20
PO_4^-	0.81 ± 0.01, n = 12	0.81 ± 0.03, n = 23	0.8 ± 0.04, n = 22	0.79 ± 0.05, n = 20
N:P	15.47	15.27	15.23	14.98
Si	4.7 ± 0.03, n = 12	4.57 ± 0.22, n = 23	4.48 ± 0.34, n = 22	4.18 ± 0.53, n = 20
N:Si	2.68	2.71	2.71	2.84
DOC	51.1 ± 0.44, n = 20	52.47 ± 2.27, n=18	51.96 ± 2.03, n = 17	51.99 ± 0.64, n = 16
TDN	15.62 ± 0.51, n = 14	15.45 ± 0.28, n = 18	14.69 ± 1.79, n = 17	15.1 ± 0.56, n = 16
		——Below mixed layer——		
NO_3^-	14.57 ± 1.42, n = 4	15.62 ± 1.38, n = 13	16.12 ± 1.76, n = 15	15.71 ± 1.04, n = 19
PO_4^-	0.95 ± 0.1, n = 4	1.04 ± 0.09, n = 13	1.05 ± 0.11, n = 15	1.04 ± 0.11, n = 19
N:P	15.38	15.08	15.36	15.1
Si	6.94 ± 1.65, n = 4	8.08 ± 1.69, n = 13	8.26 ± 1.95, n = 15	8.55 ± 1.98, n = 19
N:Si	2.1	1.93	1.95	1.84
DOC	49.59 ± 0.59, n = 8	49.92 ± 0.53, n = 9	48.35 ± 0.37, n = 10	50.58 ± 0.24, n = 10
TDN	18.7 ± 0.97, n = 8	19.15± 1.44, n = 9	19.64 ± 1.54, n = 10	19.39 ± 1.44, n = 10

Norwegian Basin	1st visit	2nd visit	3rd visit
MLD	43 m	37 m	56 m
NO_3^-	12.34 ± 0.24, n = 11	13.13 ± 0.37, n = 7	12.45 ± 0.39, n = 14
PO_4^-	0.81 ± 0.01, n = 11	0.83 ± 0.01, n = 7	0.83 ± 0.03, n = 14
N:P	15.24	15.82	15
Si	5.36 ± 0.05, n = 11	5.47 ± 0.15, n = 7	5.68 ± 0.17, n = 14
N:Si	2.3	2.4	2.19
DOC	51.64 ± 1.44, n = 7	51.72 ± 0.81, n = 7	51.34 ± 0.33, n = 18
TDN	15.79 ± 3.0, n = 7	15.43 ± 2.41, n = 7	16.60 ± 1.13, n = 10
——**Below mixed layer**———			
NO_3^-	13.08 ± 0.96, n = 30	14.12 ± 0.9, n = 48	16.59 ± 1.03, n = 46
PO_4^-	0.88 ± 0.08, n = 30	0.93 ± 0.07, n = 48	0.93 ± 0.07, n = 46
N:P	14.86	15.18	17.84
Si	6.61 ± 2.04, n = 30	7.31 ± 2.13, n = 48	7.28 ± 2.13, n = 46
N:Si	1.98	1.93	2.28
DOC	50.38 ± 2.14, n = 18	50.24 ± 1.04, n = 22	49.70 ± 0.86, n = 18
TDN	14.33 ± 2.04, n = 18	15.41 ± 2.69, n = 22	16.44 ± 1.81, n = 18

Shetland Shelf	1st visit	2nd visit
MLD	100 m	100 m
NO_3^-	9.46 ± 0.06, n = 7	8.54 ± 0.24, n = 22
PO_4^-	0.62 ± 0.01, n = 7	0.57 ± 0.02, n = 22
N:P	15.26	14.98
Si	2.83 ± 0.03, n = 7	1.71 ± 0.29, n = 22
N:Si	3.34	4.99
DOC	52.54 ± 2.25, n = 13	54.36 ± 0.42, n = 6
TDN	12.74 ± 0.26, n = 13	12.60 ± 0.27, n = 6
——**Below mixed layer**———		
NO_3^-	9.33 ± 0.05, n = 4	8.85 ± 0.27, n = 6
PO_4^-	0.63 ± 0.01, n = 4	0.62 ± 0.04, n = 6
N:P	14.81	14.27
Si	2.78 ± 0.06, n = 4	2.24 ± 0.17, n = 6
N:Si	3.36	3.95
DOC	53.51 ± 0.78, n = 5	54.36 ± 0.42, n = 6
TDN	12.99 ± 0.51, n = 5	12.93 ± 0.16, n = 6

Supplementary 2

Iceland Basin

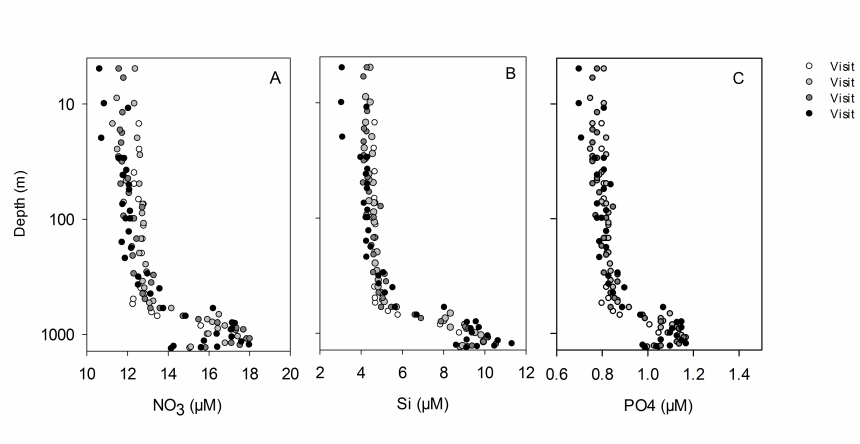

Norwegian Basin

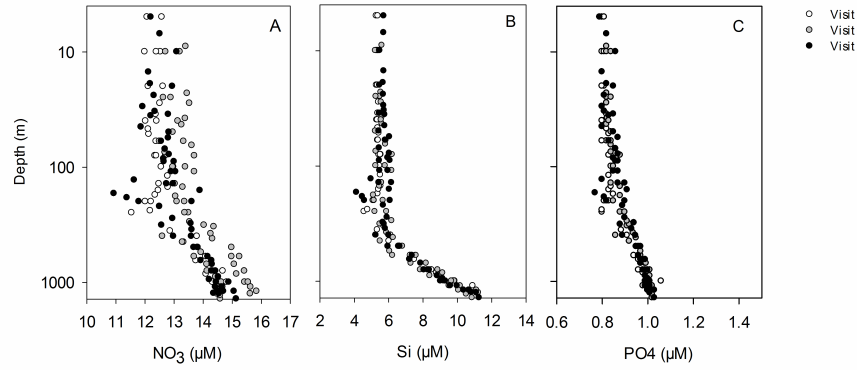

Shetland Shelf

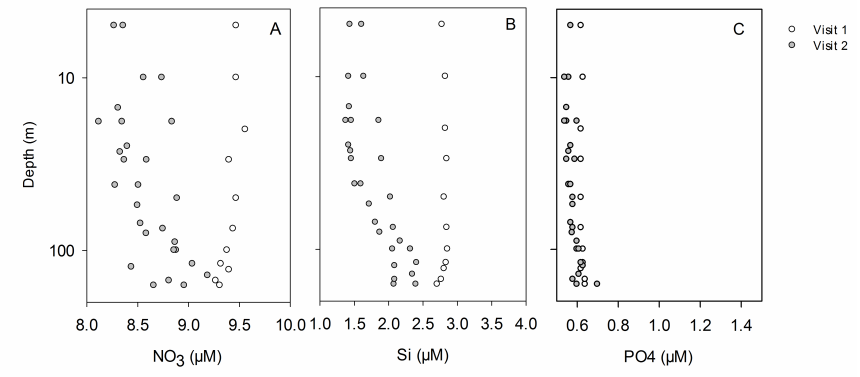

Figure 13: Nutrient profiles N, P and Si (µM) at each station throughout the investigated period.

Supplementary 3

Vertical profiles (log-log scale) of heterotrophic and autotrophic cells ml^{-1} at the three stations.

Dashed lines indicate the mixed layer depth.

Iceland Basin

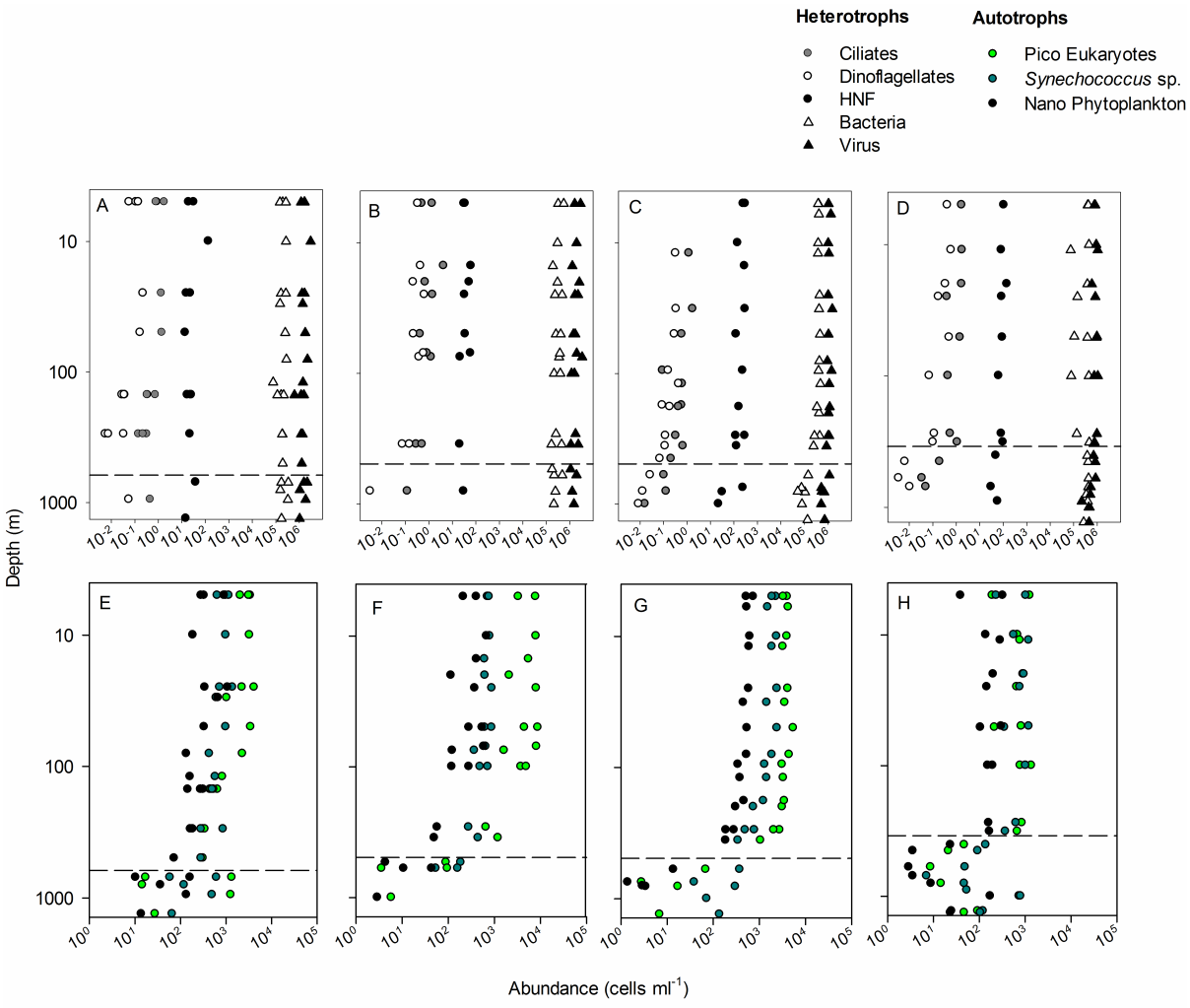

Norwegian Basin

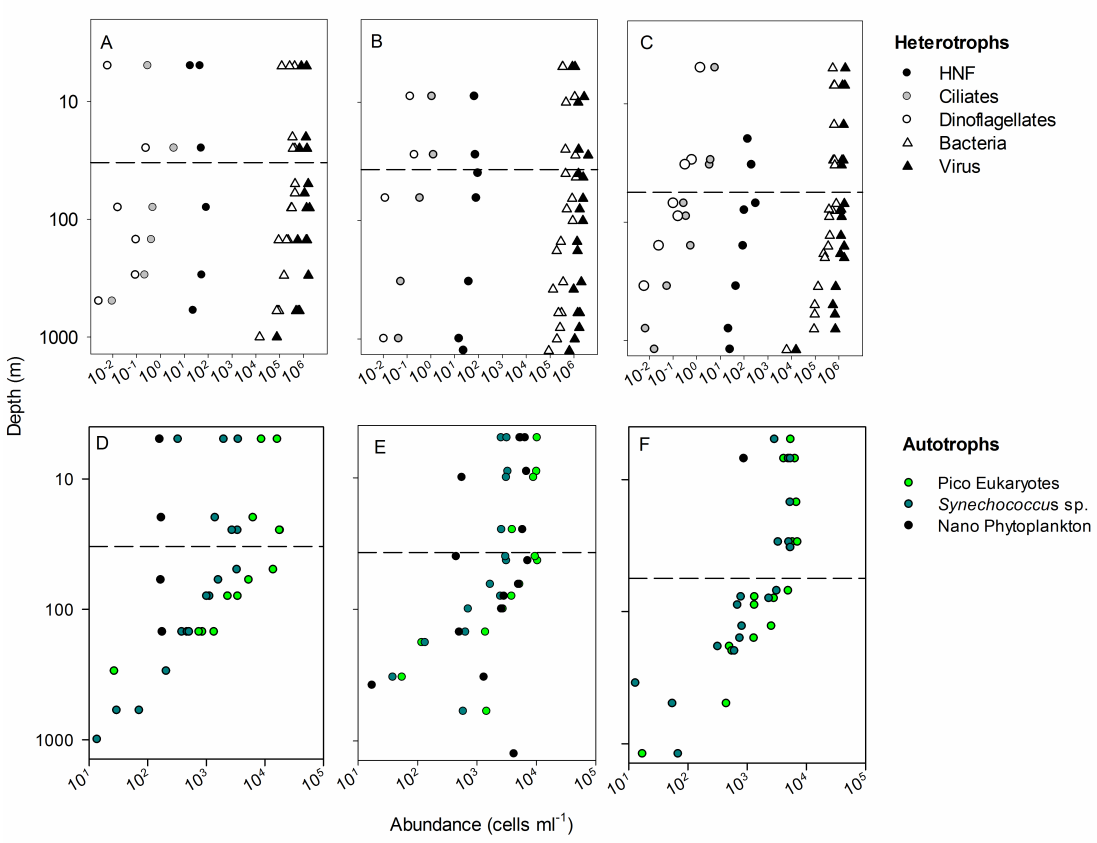

Shetland Shelf

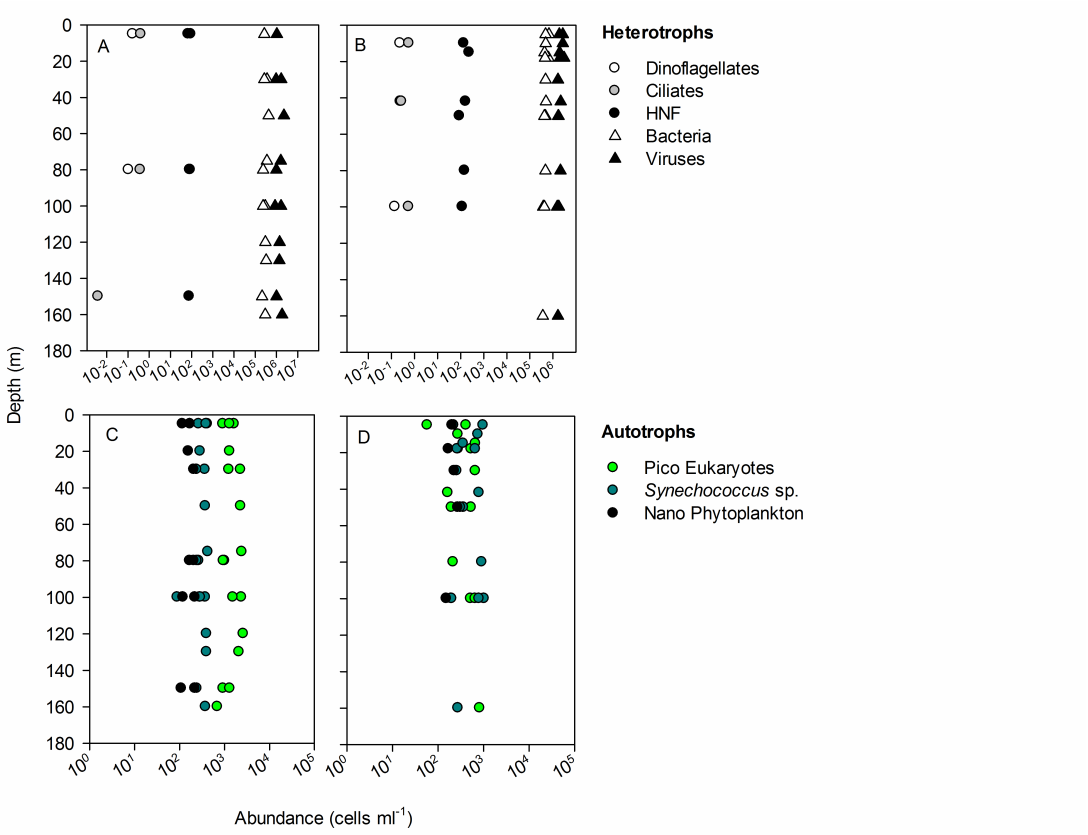

Supplementary 4

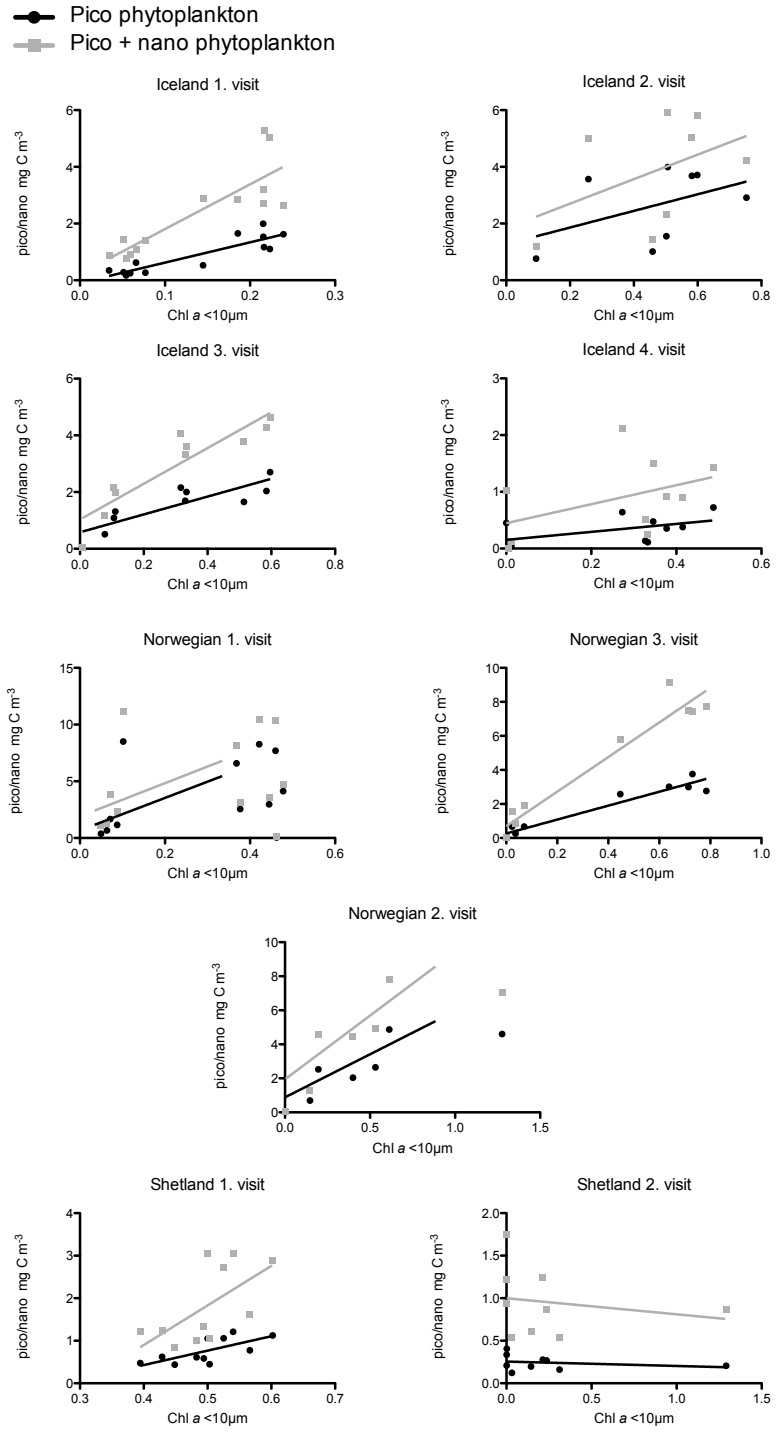

Figure 14: Linear regression made on the correlations of Chl $a < 10$ µm and the biomass of pico- and nanophytoplankton at each visit to each station. See slope and P value, for those with P value $<$ 0.05 in table 2, 3, 4.

Supplementary 5

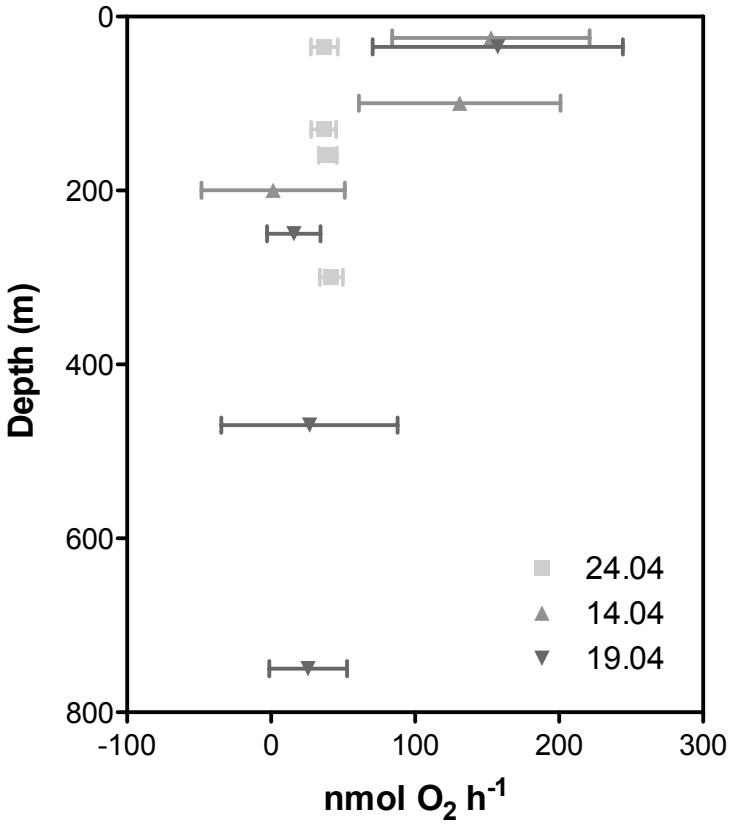

Figure 15: Bacterial respiration shown as mean ± SD of 6 replicates. Measurements were taken continuously every 12 h for 36 h with a oxygen-optode (at 6 °C). Depths of sampled water at the Iceland Basin and dates as given in the figure.

Supplementary 6

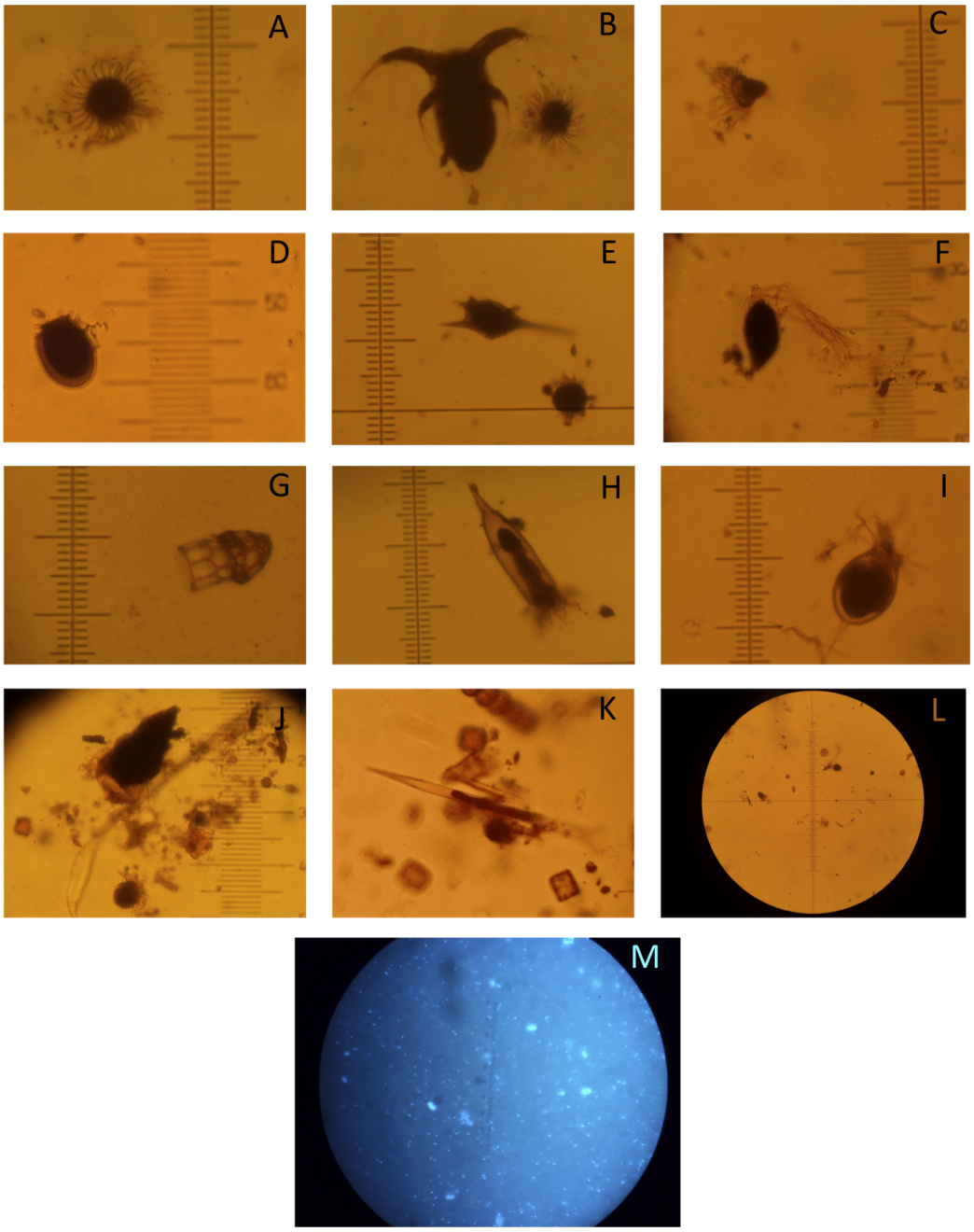

Figure 16: Microscope images. Organisms are not selected after relative abundance. **A**: *Strobilidium oviformis* **B**: *Strombidium* spp. and copepod nauplii. **C**: *Strobilidium* spp. **D**: *Dinophysis* spp. **E**: *Ceratium* spp. (armored dinoflagellate) and *Mesodinium* spp. **F**: *Gyrodinium spirale* (naked dinoflagellate). **G-I**: Tintinnids (lorica forming ciliates), G: empty lorica. **J**: *Strombidium* spp. **K**: Tintinnid and chain forming *Chaetoceros* spp.. **L**: Example of a relatively empty surface sample from fist visit at the Iceland Basin. **M**: images from epifluorescence microscope, the relatively larger cells presenting nano flagellates. As size reference for images A-L, each line segment is equivalent to 5µm; for image M each segment is 1µm. All pictures taken by Maria Lund Paulsen.

Supplementary 7

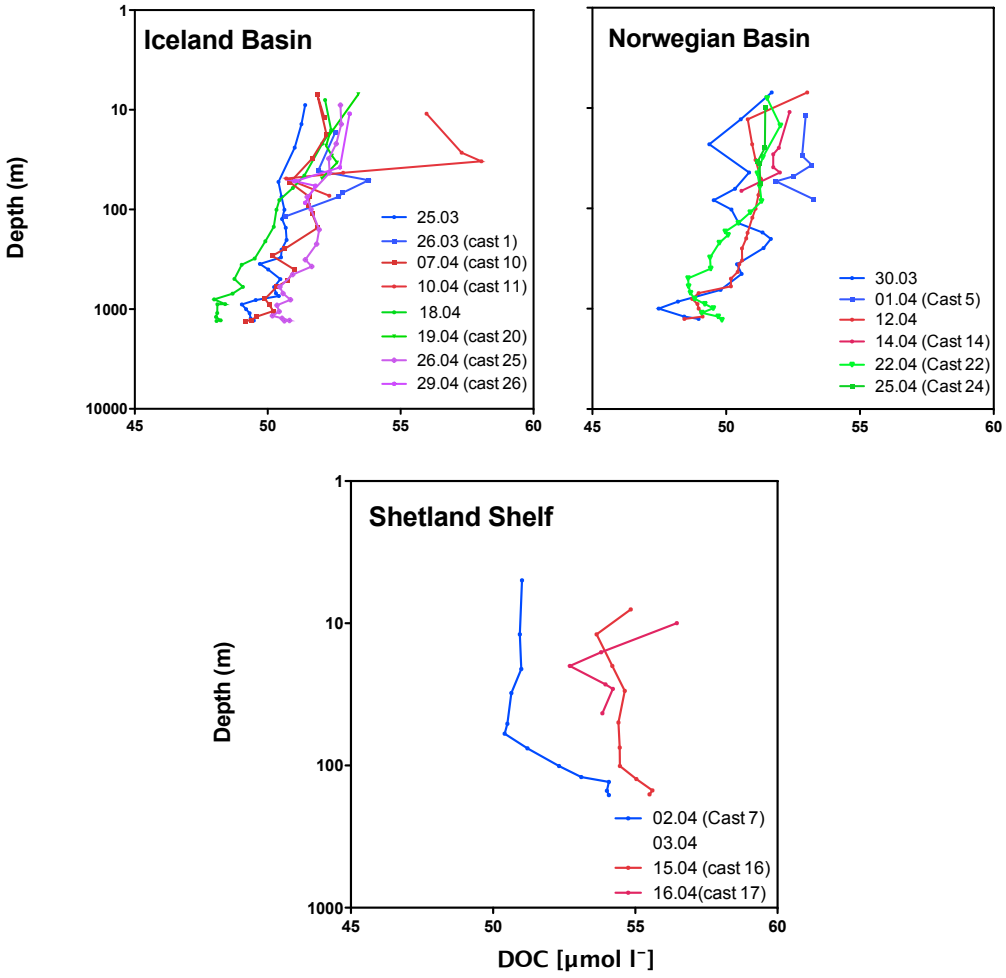

Figure 17: Vertical profiles of DOC measured at the three stations (log scale).